Reliability analysis of structures with interval uncertainties under stationary stochastic excitations

RELIABILITY ANALYSIS OF STRUCTURES WITH INTERVAL UNCERTAINTIES UNDER STATIONARY STOCHASTIC EXCITATIONS

GIUSEPPE MUSCOLINO[1], ROBERTA SANTORO[2] and ALBA SOFI[3,*]

[1]*Department of Engineering and Inter-University Centre of Theoretical and Experimental Dynamics, University of Messina, Villaggio S. Agata, 98166 Messina, Italy. E-mail: gmuscolino@unime.it*

[2]*Department of Engineering, University of Messina, Villaggio S. Agata, 98166 Messina, Italy. E-mail: roberta.santoro@unime.it*

[3]*Department of Civil, Energy, Environmental and Materials Engineering and Inter-University Centre of Theoretical and Experimental Dynamics, University Mediterranea of Reggio Calabria, Via Graziella, Feo di Vito, 89124 Reggio Calabria Italy. E-mail: alba.sofi@unirc.it*

Reliability analysis of linear discretized structural systems with interval uncertainties subjected to stationary Gaussian random excitation is addressed. Under the assumption of independent up-crossings of a specified threshold, an efficient procedure for the evaluation of the bounds of the *interval reliability function* of the generic response process is presented. The first step of the proposed approach is to derive approximate expressions of the interval mean-value and spectral moments of the response along with the associated bounds. To this aim, the *improved interval analysis via extra unitary interval* is applied in conjunction with a novel series expansion of the inverse of an interval matrix with modifications, called *Interval Rational Series Expansion* (*IRSE*). Then, the lower bound and upper bounds of the *interval reliability function* are readily evaluated by properly combining the bounds of the interval mean-value and spectral moments of the response. Two numerical examples are provided to demonstrate the accuracy of the proposed procedure and its usefulness in view of decision-making in engineering practice.

Keywords: Interval uncertainties; Stochastic excitation; Reliability analysis; Interval Rational Series Expansion; Improved interval analysis; Upper bound and lower bound.

*Corresponding author

1 INTRODUCTION

Reliability assessment of randomly excited structural systems with uncertain parameters is of crucial importance to guarantee prescribed safety requirements for real structures under environmental loads, such as earthquake ground motion, sea waves or gusty winds (see e.g. [1-3]).

Uncertainties affecting structural parameters have traditionally been modeled in the context of the classical probability theory as random variables or random fields. Well-established probabilistic methods have been developed to analyze the effects of uncertainties on structural performance. However, available data are often insufficient to build credible probabilistic distributions of the uncertain parameters, especially in early design stages. The selection of the probability density function (*PDF*) which represents best an uncertain parameter then involves subjective decisions made by the analyst. The main drawback in the context of reliability analysis is the high sensitivity of the probabilities of failure to small variations of the assumed probabilistic models [4,5]. Over the last decade, a number of non-probabilistic approaches [6] have gained much popularity as alternative tools for quantifying and processing uncertainties described by fragmentary or incomplete data. In this context, the interval model, originally developed on the basis of the interval analysis [7,8], is widely used when only bounds are known for the parameters involved in the engineering problem. This model does not provide any information on the frequency of occurrence of values between the lower and upper bounds. The analysis of structures with interval basic input parameters is thus oriented to estimate the range of variation of the response quantities. If only scarce information is available, a range of possible values appears more credible than a crisp value of the response provided by a probabilistic analysis based on subjective decisions.

After the pioneering study by Ben-Haim [4], who first introduced a non-probabilistic concept of reliability, a growing interest has arisen in structural safety assessment based on non-traditional uncertainty models [9-20]. Recently, interpretations [21], comparisons [22] and combinations [23-26] of alternative uncertainty representations in the context of reliability analysis have also been presented.

To the best of the authors' knowledge, studies on reliability analysis of structures with uncertain parameters modeled within a non-probabilistic context mainly covered the static analysis, while only a few contributions dealing with random excitations are available. Ma et al. [27] developed a new two-factor method based on the probability and the fuzzy sets theory for the analyses of the dynamic response and reliability of fuzzy-random truss systems under stationary stochastic excitation. Within the interval framework, due to structural parameters uncertainty, the statistics of the random response as well as the reliability function of randomly excited structures turn out to have an interval nature, say they range between a lower bound and an upper bound rather than assuming a given value. In this context, the aim of structural safety assessment is the evaluation of the lower bound and upper bound of the interval reliability of the selected response process. From an engineering point of view, such bounds provide information on the range of structure's performance useful for decision-making. Interval reliability analysis poses serious challenges since all possible combinations arising between the lower bound and upper bound of the uncertain parameters need to be explored. The *vertex method* (see e.g., [28]) is considered the most robust approach, but the associated computational cost increases exponentially with the number of uncertainties. Indeed, for N uncertain parameters, the *vertex method* requires 2^N analyses, as many as are the combinations of the extreme values of the N input intervals. Therefore, there is a need to develop alternative methods able to explore the entire range of interval uncertainties while keeping computational costs relatively low. Within the framework of the widely used first-passage failure model [29,30], the authors [31] derived approximate expressions of reliability sensitivities for structures with uncertain-but-bounded parameters subjected to stationary Gaussian random excitation. For small uncertainty levels, accurate estimates of the bounds of the *interval reliability function* have been obtained by applying the *first-order interval Taylor series expansion.* Recently, Do et al. [32] evaluated the range of dynamic reliability of structures with interval parameters and safe bounds under stationary random excitation by applying an improved particle swarm optimization algorithm.

This study presents an efficient method for structural reliability assessment of linear discretized structures with interval parameters subjected to stationary Gaussian random excitation. The probability of failure is identified with the first passage probability, under the Poisson assumption of independent up-crossings [29,30]. The proposed procedure relies on the observation that the *interval reliability function* depends on three interval quantities: the interval mean-value and spectral moments of zero- and second-order of the stationary random response process. Then, the lower bound and upper bound of the *interval reliability function* of the selected response process can be derived as corresponding to appropriate combinations of the bounds of the interval mean-value and spectral moments. Such bounds are evaluated in approximate form by applying the *improved interval analysis via extra unitary interval* [33] in conjunction with the so-called *Interval Rational Series Expansion* (*IRSE*) [34-36] for deriving the explicit approximate inverse of an interval matrix with small rank r modifications. In order to apply the *IRSE*, a spectral decomposition of the interval stiffness matrix is performed. By inspection of the analytical expression of the *interval reliability function*, it is found that only four combinations of the bounds of interval response statistics need to be explored, regardless of the number of uncertain parameters. This implies that the proposed procedure exhibits substantial computational advantages over the *vertex method* and is applicable to complex structural systems with a large number of interval input variables.

To assess the accuracy and computational efficiency of the proposed method, reliability analysis of a truss structure and a chimney with interval Young's modulus under wind excitation is performed. Appropriate comparisons with the *vertex method* solutions are presented. Furthermore, interpretation of numerical results from an engineering perspective and their usefulness for decision-making are discussed.

The paper is organized as follows. In Section 2, the problem formulation is presented and the fundamentals of the *improved interval analysis via extra unitary interval* are given. Then, the concept of interval structural reliability is introduced in Section 3. In Section 4, approximate

expressions of the bounds of the interval mean-value and spectral moments of the stationary response are derived. Section 5 presents an efficient procedure for the evaluation of the bounds of the *interval reliability function*. Finally, in Section 6 two numerical examples are provided to show the accuracy and computational efficiency of the proposed method.

2 LINEAR STRUCTURE WITH INTERVAL UNCERTAINTIES UNDER STOCHASTIC EXCITATION

2.1 Interval Uncertainty Modeling

The interval model, originally developed from the interval analysis [7], is a widely used non-probabilistic approach to handle uncertainties occurring in engineering problems. The underlying idea is to represent the generic uncertain parameter as an interval variable ranging between its lower and upper bounds. Denoting by $\mathbb{IR}$ the set of all closed real interval numbers, let $\boldsymbol{\alpha}^I = \left[\underline{\boldsymbol{\alpha}}, \overline{\boldsymbol{\alpha}}\right] \in \mathbb{IR}^r$ be a bounded set-interval vector of real numbers such that $\underline{\boldsymbol{\alpha}} \le \boldsymbol{\alpha} \le \overline{\boldsymbol{\alpha}}$. The apex I means interval variable, while the symbols $\underline{\boldsymbol{\alpha}}$ and $\overline{\boldsymbol{\alpha}}$ denote the lower bound (*LB*) and upper bound (*UB*) vectors. According to the *classical interval arithmetic*, the i-th real interval variable $\alpha_i^I = \left[\underline{\alpha}_i, \overline{\alpha}_i\right]$ is characterized by the midpoint value (or mean), $\alpha_{0,i}$, and the deviation amplitude (or radius), $\Delta\alpha_i$, given by:

$$\alpha_{0,i} = \mathrm{mid}\left\{\alpha_i^I\right\} = \frac{1}{2}\left(\underline{\alpha}_i + \overline{\alpha}_i\right); \quad \Delta\alpha_i = \frac{1}{2}\left(\overline{\alpha}_i - \underline{\alpha}_i\right) \tag{1a,b}$$

where $\mathrm{mid}\{\bullet\}$ denotes the midpoint of the interval quantity between curly brackets.

The real numbers $\alpha_i \in \alpha_i^I = \left[\underline{\alpha}_i, \overline{\alpha}_i\right]$, collected into the vector $\boldsymbol{\alpha} \in \boldsymbol{\alpha}^I = \left[\underline{\boldsymbol{\alpha}}, \overline{\boldsymbol{\alpha}}\right]$, are here assumed to represent the dimensionless fluctuations of the uncertain structural parameters around their midpoint values. In the sequel, $\boldsymbol{\alpha}_0$ and $\Delta\boldsymbol{\alpha}$ will denote the vectors listing the midpoint values (or

mean values) and the deviation amplitudes (or radii), $\alpha_{0,i}$ and $\Delta\alpha_i$, respectively, of the interval parameters α_i^I $(i=1,2,...,r)$.

The main drawback of the *classical interval analysis* is the so-called *dependency phenomenon* [8] which often leads to an overestimation of the interval solution width unacceptable from an engineering point of view. This occurs when an expression contains multiple instances of one or more interval variables due to the inability of the classical interval arithmetic to keep track of the dependency between interval variables throughout calculations. To limit the effects of the *dependency phenomenon*, recently the so-called *improved interval analysis via extra unitary interval* has been proposed [33]. The key feature of this approach is the introduction of the *extra unitary interval* (*EUI*), $\hat{e}_i^I=\left[-1,+1\right]$, $(i=1,2,...,r)$, which does not follow the rules of the *classical interval analysis*. Indeed, the *EUI* is defined in such a way that the following properties hold:

$$\begin{aligned}
&\hat{e}_i^I-\hat{e}_i^I=0;\quad \hat{e}_i^I\times\hat{e}_i^I=\left(\hat{e}_i^I\right)^2=\left[1,1\right];\\
&\hat{e}_i^I/\hat{e}_i^I=\left[1,1\right];\quad \hat{e}_i^I\times\hat{e}_j^I=\left[-1,+1\right],\quad i\neq j;\\
&x_i\hat{e}_i^I\pm y_i\hat{e}_i^I=\left(x_i\pm y_i\right)\hat{e}_i^I;\\
&x_i\hat{e}_i^I\times y_i\hat{e}_i^I=x_iy_i\left(\hat{e}_i^I\right)^2=x_iy_i\left[1,1\right].
\end{aligned}\qquad \text{(2a-f)}$$

In these equations, $[1,1]=1$ is the so-called unitary *thin interval*. It is recalled that a thin interval occurs when $\underline{x}=\overline{x}$ and it is defined as $x^I=[\underline{x},\underline{x}]$, so that $x\in\mathbb{R}$. Notice that the *EUI* is different from the *classical unitary interval* $e^I=[-1,+1]$ which does not satisfy Eqs. (2a-f).

The *improved interval analysis via EUI* assumes the following *affine form* definition for the i-th interval parameter α_i^I:

$$\alpha_i^I=\alpha_{0,i}+\Delta\alpha_i\hat{e}_i^I,\qquad (i=1,2,\ldots,r). \tag{3}$$

It is worth emphasizing that the subscript *i* means that the *EUI*, $\hat{e}_i^I$, is associated to the *i*-th interval variable. This implies that each interval variable is characterized by a different *EUI*, so that dependencies can be duly taken into account throughout calculations.

In the framework of interval symbolism, a generic interval-valued function f and a generic interval-valued matrix function $\mathbf{A}$ of the interval vector $\boldsymbol{\alpha}^I$ will be denoted in equivalent form, respectively, as:

$$\begin{aligned} f^I &\equiv f(\boldsymbol{\alpha}^I) \Leftrightarrow f(\boldsymbol{\alpha}), \quad \boldsymbol{\alpha} \in \boldsymbol{\alpha}^I = \left[\underline{\boldsymbol{\alpha}}, \overline{\boldsymbol{\alpha}}\right]; \\ \mathbf{A}^I &\equiv \mathbf{A}(\boldsymbol{\alpha}^I) \Leftrightarrow \mathbf{A}(\boldsymbol{\alpha}), \quad \boldsymbol{\alpha} \in \boldsymbol{\alpha}^I = \left[\underline{\boldsymbol{\alpha}}, \overline{\boldsymbol{\alpha}}\right]. \end{aligned} \tag{4a,b}$$

2.2 Equations of Motion

Let us consider a quiescent *n*-DOF linear structure with uncertain-but-bounded parameters subjected to a stationary multi-correlated Gaussian stochastic process $\mathbf{f}(t)$. The equations of motion can be cast in the following form:

$$\mathbf{M}_0 \ddot{\mathbf{u}}^I(t) + \mathbf{C}^I \dot{\mathbf{u}}^I(t) + \mathbf{K}^I \mathbf{u}^I(t) = \mathbf{f}(t) \tag{5}$$

where $\mathbf{M}_0$ is the $n \times n$ mass matrix, herein assumed deterministic; $\mathbf{C}^I \equiv \mathbf{C}(\boldsymbol{\alpha}^I)$ and $\mathbf{K}^I \equiv \mathbf{K}(\boldsymbol{\alpha}^I)$ are the $n \times n$ damping and stiffness matrices of the structure which depend on the dimensionless interval parameters collected into the vector $\boldsymbol{\alpha} \in \boldsymbol{\alpha}^I$ of order *r*; $\mathbf{u}^I(t) \equiv \mathbf{u}(\boldsymbol{\alpha}^I, t)$ is the stationary Gaussian vector process of displacements; and a dot over a variable denotes differentiation with respect to time t. The Rayleigh model is herein adopted for the interval damping matrix, i.e.:

$$\mathbf{C}^I = c_0 \mathbf{M}_0 + c_1 \mathbf{K}^I \tag{6}$$

where c_0 and c_1 are the Rayleigh damping constants having units s^{-1} and s, respectively. For the sake of simplicity, in the present study, the constants c_0 and c_1 are taken coincident with those pertaining to the nominal structure.

In structural engineering, the dimensionless fluctuations of the uncertain-but-bounded parameters around their nominal values can be reasonably modelled as symmetric intervals, i.e. $\alpha_i^I \in \left[\underline{\alpha}_i, \overline{\alpha}_i\right]$ with $\overline{\alpha}_i = -\underline{\alpha}_i$, so that $\alpha_{0,i} = 0$ and $\Delta\alpha_i = \overline{\alpha}_i = -\underline{\alpha}_i$. Under this assumption, Eq. (3) reduces to:

$$\alpha_i^I = \Delta\alpha_i \hat{e}_i^I. \tag{7}$$

Furthermore, to assure physically meaningful values of the uncertain structural properties, the deviation amplitudes $\Delta\alpha_i$ should satisfy the conditions $\Delta\alpha_i < 1$. For instance, if the uncertain Young's modulus of the i-th structural element is expressed as $E_i^I = E_{0,i}\left(1 + \Delta\alpha_i \hat{e}_i^I\right)$, with $E_{0,i}$ denoting the nominal value, the fluctuation α_i^I defined by Eq. (7) must satisfy the condition $\Delta\alpha_i < 1$ to yield always positive values of the interval material property.

The external load vector $\mathbf{f}(t)$ in Eq. (5), modelled here as a stationary multi-correlated Gaussian random process, is fully characterized, from a probabilistic point of view, by the mean-value vector, $\boldsymbol{\mu}_\mathbf{f} = \mathrm{E}\langle \mathbf{f}(t) \rangle$, and the correlation function matrix, $\mathbf{R}_{\mathbf{ff}}(t_2 - t_1) = \mathbf{R}_{\mathbf{ff}}(\tau) = \mathrm{E}\left\langle \mathbf{f}(t_1)\mathbf{f}^{\mathrm{T}}(t_2) \right\rangle - \boldsymbol{\mu}_\mathbf{f}\, \boldsymbol{\mu}_\mathbf{f}^{\mathrm{T}}$, with $\mathrm{E}\langle \bullet \rangle$ denoting the stochastic average operator.

The interval stationary Gaussian stochastic response process $\mathbf{u}^I(t)$ of structures with uncertain-but-bounded parameters is completely characterized in the frequency domain by the interval mean-value vector, $\boldsymbol{\mu}_\mathbf{u}^I \equiv \boldsymbol{\mu}_\mathbf{u}(\boldsymbol{\alpha}^I)$, and the interval Power Spectral Density (*PSD*) function matrix, $\mathbf{G}_{\mathbf{uu}}^I(\omega) \equiv \mathbf{G}_{\mathbf{uu}}(\boldsymbol{\alpha}^I, \omega)$, [34]. As known, the generic response quantity of practical interest, $Y^I(t) \equiv Y(\boldsymbol{\alpha}^I, t)$ (e.g. displacement, strain or stress at a critical point), can be determined from the displacement vector $\mathbf{u}^I(t)$ by means of the following relationship:

$$Y^I(t) = \mathbf{q}^{\mathrm{T}}\, \mathbf{u}^I(t) \tag{8}$$

where $\mathbf{q}$ is a vector collecting the combination coefficients relating the response process $Y^I(t)$ to $\mathbf{u}^I(t)$. Depending on the selected response quantity, the vector $\mathbf{q}$ in Eq. (8) may depend on the uncertain parameters; such dependency is here omitted for the sake of simplicity.

The complete probabilistic characterization of the interval stationary Gaussian random process, $Y^I(t) = \mu_Y^I + \tilde{Y}^I(t)$, requires the knowledge of the interval mean-value, μ_Y^I, and the interval *PSD* function, $G_{\tilde{Y}\tilde{Y}}^I(\omega) \equiv G_{YY}^I(\omega)$ of the zero-mean random process $\tilde{Y}^I(t)$.

The interval mean-value, μ_Y^I, that, without loss of generality, is herein assumed positive $(\mu_Y^I > 0)$, can be evaluated taking the stochastic average of both sides of Eq. (8), i.e.:

$$\mu_Y^I = \mathrm{E}\left\langle Y^I(t)\right\rangle = \mathbf{q}^{\mathrm{T}}\boldsymbol{\mu}_{\mathbf{u}}^I = \mathbf{q}^{\mathrm{T}}\left(\mathbf{K}^I\right)^{-1}\boldsymbol{\mu}_{\mathbf{f}} \tag{9}$$

where $\boldsymbol{\mu}_{\mathbf{u}}^I$ is the interval mean-value of the displacement vector $\mathbf{u}^I(t)$.

Based on Eq. (8), the interval *PSD* function of the zero-mean response process $\tilde{Y}^I(t)$ reads:

$$G_{\tilde{Y}\tilde{Y}}^I(\omega) = \mathbf{q}^{\mathrm{T}}\mathbf{G}_{\mathbf{uu}}^I(\omega)\mathbf{q} = \mathbf{q}^{\mathrm{T}}\mathbf{H}^*(\boldsymbol{\alpha}^I,\omega)\mathbf{G}_{\tilde{\mathbf{X}}_\mathbf{f}\tilde{\mathbf{X}}_\mathbf{f}}(\omega)\mathbf{H}^{\mathrm{T}}(\boldsymbol{\alpha}^I,\omega)\mathbf{q} \equiv G_{YY}^I(\omega) \tag{10}$$

where the asterisk means complex conjugate; $\mathbf{G}_{\tilde{\mathbf{X}}_\mathbf{f}\tilde{\mathbf{X}}_\mathbf{f}}(\omega)$ is the *PSD* function matrix of the zero-mean stationary Gaussian stochastic process, $\tilde{\mathbf{X}}_\mathbf{f}(t)$, describing the random fluctuation of the input process, i.e. $\mathbf{f}(t) = \boldsymbol{\mu}_\mathbf{f} + \tilde{\mathbf{X}}_\mathbf{f}(t)$; $\mathbf{H}^I(\omega) \equiv \mathbf{H}(\boldsymbol{\alpha}^I,\omega)$ is the interval *frequency response function* (*FRF*) matrix (also referred to as *transfer function matrix*), defined as:

$$\mathbf{H}^I(\omega) \equiv \mathbf{H}(\boldsymbol{\alpha}^I,\omega) = \left[-\omega^2\mathbf{M}_0 + \mathrm{j}\omega\mathbf{C}^I + \mathbf{K}^I\right]^{-1} \tag{11}$$

with $\mathrm{j} = \sqrt{-1}$ denoting the imaginary unit.

3 INTERVAL RELIABILITY FUNCTION

The probability of failure for structural systems subjected to stochastic excitations is commonly identified with the *first passage probability*, i.e. the probability that the *extreme value* random process, $Y^I_{\max}(T) \equiv Y_{\max}(\boldsymbol{\alpha}^I, T)$, for the generic structural response process of interest, $Y^I(t)$, firstly exceeds the safety bounds within a specified time interval $[0,T]$. For a structure with uncertain-but-bounded parameters, the *extreme value* random process, over a time interval $[0,T]$, is mathematically defined as:

$$Y_{\max}(\boldsymbol{\alpha},T) = \max_{0\le t\le T} \left|Y(\boldsymbol{\alpha},t)\right|,\ \boldsymbol{\alpha} \in \boldsymbol{\alpha}^I = \left[\underline{\boldsymbol{\alpha}}, \overline{\boldsymbol{\alpha}}\right] \tag{12}$$

where the symbol $|\bullet|$ denotes absolute value.

It can be easily shown that the *cumulative distribution function* (*CDF*) of the *extreme value* random process, $Y^I_{\max}(T)$, also called *reliability function*, $L^I_{Y_{\max}}(b,T)$, formally coincides with the *CDF* of the zero-mean random process $\tilde{Y}^I_{\max}(T) = \max_{0\le t\le T}\left|\tilde{Y}^I(t)\right|$. The *CDF*, $L^I_{Y_{\max}}(b,T)$, represents the probability that the random process $Y^I_{\max}(T) - \mu^I_Y$ is equal to or less than the barrier level $b - \mu^I_Y$ within the time interval $[0,T]$ and it is commonly expressed as [37]:

$$L^I_{Y_{\max}}(b,T) = \mathcal{P}\left[Y^I_{\max}(T) - \mu^I_Y \le b - \mu^I_Y\right] = P^I_{0,Y}(b)\exp\left[-T\ \eta^I_Y(b)\ \right] \tag{13}$$

where $P^I_{0,Y}(b) = \mathcal{P}[Y^I_{\max}(0) - \mu^I_Y \le b - \mu^I_Y]$ denotes the initial probability, that is the probability of not exceeding the level $b - \mu^I_Y$ at time $t = 0$; $\eta^I_Y(b)$ is the so-called *hazard function* (or *intensity function* or *limiting decay rate*). The latter provides the conditional occurrence rate of up-crossings at time *t* of the level $b - \mu^I_Y$ by the random process $\left|Y^I(t)\right| - \mu^I_Y$, given that this level has not been up-crossed prior to *t*.

In the case of randomly excited structural systems with interval uncertain parameters, the *CDF* of the *extreme value* random process, $Y^I_{\max}(T)$, turns out to be an interval function i.e.:

$$L^I_{Y_{\max}}(b,T) = \left[\underline{L}_{Y_{\max}}(b,T), \overline{L}_{Y_{\max}}(b,T) \right] \tag{14}$$

where $\underline{L}_{Y_{\max}}(b,T)$ and $\overline{L}_{Y_{\max}}(b,T)$ are the *LB* and *UB* of $L^I_{Y_{\max}}(b,T)$, respectively.

Since the *hazard function* $\eta^I_Y(b)$ (see Eq. (13)) is not available in exact form, different approximate expressions have been proposed in the literature (see e.g., [29]). It is recognized that, if the failure level is high enough, then the classical Rice's formula, based on the Poisson assumption of independent up-crossings [38], is applicable. In this case, the *hazard function* $\eta^I_Y(b)$, for Gaussian processes with sufficiently large mean-value, $\mu^I_Y > 0$, can be assumed, with good accuracy, as coincident with the mean up-crossing rate of a single barrier $b - \mu^I_Y$ [37]. Then, the interval *CDF*, $L^I_{Y_{\max}}(b,T)$, can be expressed as:

$$L^I_{Y_{\max}}(b,T) \approx P^I_{0,Y}(b) \exp\left[-T\ \nu^+_Y(\boldsymbol{\alpha}^I) \exp\left(-\frac{(b-\mu^I_Y)^2}{2\lambda^I_{0,Y}} \right) \right] \tag{15}$$

where

$$\nu^+_Y(\boldsymbol{\alpha}^I) \equiv \nu^{+I}_Y = \frac{1}{2\,\pi} \sqrt{\frac{\lambda_{2,Y}(\boldsymbol{\alpha}^I)}{\lambda_{0,Y}(\boldsymbol{\alpha}^I)}} \tag{16}$$

is the mean up-crossing rate at level $\mu^I_Y > 0$; $P^I_{0,Y}(b)$ represents the initial interval probability, herein assumed equal to unity; $\lambda^I_{0,Y} \equiv \lambda^I_{0,\tilde{Y}}$ and $\lambda^I_{2,Y} \equiv \lambda^I_{2,\tilde{Y}}$ are the zero- and second-order interval spectral moments which represent the variance of the process $Y^I(t)$ and of its derivative $\dot{Y}^I(t)$, respectively. By applying interval extension, the interval spectral moments of order j of the random process $\tilde{Y}^I(t)$, which are the same as those of $Y^I(t)$, are defined as follows [39]:

$$\lambda^I_{j,\tilde{Y}} \equiv \lambda^I_{j,Y} = 2\int_0^\infty \omega^j\ G^I_{YY}(\omega)\,\mathrm{d}\omega, \quad j = 0, 2. \tag{17}$$

Though the structural system possesses r interval uncertain properties, α_i^I, based on Eqs. (15) and (16), the *interval reliability function* $L_{Y_{\max}}^I(b,T)$ may be viewed as depending on only three interval parameters, namely μ_Y^I, $\lambda_{0,Y}^I$ and $\lambda_{2,Y}^I$.

In the next section, the bounds of the interval mean-value and spectral moments of the interval stationary stochastic response process $Y^I(t)$, useful for deriving the region of the *interval reliability function*, $L_{Y_{\max}}^I(b,T)$, will be evaluated in approximate form.

4 APPROXIMATE INTERVAL MEAN-VALUE AND SPECTRAL MOMENTS OF THE RESPONSE PROCESS

4.1 Interval Mean-Value

The stiffness matrix of a linear-elastic structure can always be expressed as a linear function of the structural parameters, eventually by applying a suitable variable transformation [40]. Based on this observation and following the interval formalism introduced above, the $n \times n$ order interval stiffness matrix, $\mathbf{K}^I$, of the $n-$DOF structural system governed by Eq. (5) can be expressed as a linear function of the uncertain properties, i.e.:

$$\mathbf{K}^I = \mathbf{K}_0 + \sum_{i=1}^{r} \mathbf{K}_i \, \Delta\alpha_i \, \hat{e}_i^I \tag{18}$$

where

$$\mathbf{K}_0 = \mathbf{K}(\boldsymbol{\alpha})\big|_{\boldsymbol{\alpha}=\mathbf{0}}; \quad \mathbf{K}_i = \left.\frac{\partial \mathbf{K}(\boldsymbol{\alpha})}{\partial \alpha_i}\right|_{\boldsymbol{\alpha}=\mathbf{0}}. \tag{19a,b}$$

In these equations, $\mathbf{K}_0$ denotes the stiffness matrix of the nominal structural system (i.e. with $\boldsymbol{\alpha}=\mathbf{0}$) which is a positive definite symmetric matrix of order $n \times n$; $\mathbf{K}_i$ is a positive semi-definite symmetric matrix of order $n \times n$ and rank p_i; $\Delta\alpha_i$ is the dimensionless deviation amplitude of the *i*-th uncertain parameter $\alpha_i \in \alpha_i^I = \Delta\alpha_i \hat{e}_i^I$ satisfying the condition $\Delta\alpha_i < 1$.

The interval mean-value of the generic response process $\mu_Y^I = \mathrm{E}\left\langle Y^I(t)\right\rangle$ can be evaluated by applying Eq. (9) once the inverse of the interval stiffness matrix is determined. To this aim, an alternative explicit expression of the Neumann series [41,42] for evaluating the inverse of an interval matrix with small rank-r modifications, known as *Interval Rational Series Expansion* (*IRSE*) [31, 34-36] is applied. An essential step for the application of the *IRSE* is the decomposition of the deviation of the interval stiffness matrix $\mathbf{K}^I$ with respect to the nominal value $\mathbf{K}_0$ as superposition of rank-one matrices. As shown by Eq. (18), in general, the deviation is given as sum of r matrices $\mathbf{K}_i$ of rank p_i multiplied by the associated interval uncertainties $\alpha_i^I = \Delta\alpha_i \hat{e}_i^I$. Let us express the $i-$th matrix $\mathbf{K}_i$ in the following form:

$$\mathbf{K}_i = \sum_{\ell=1}^{p_i} \lambda_i^{(\ell)} \mathbf{v}_i^{(\ell)} \mathbf{v}_i^{(\ell)\mathrm{T}} \tag{20}$$

where

$$\mathbf{v}_i^{(\ell)} = \mathbf{K}_0 \boldsymbol{\psi}_i^{(\ell)} \tag{21}$$

$\boldsymbol{\psi}_i^{(\ell)}$ and $\lambda_i^{(\ell)}$ being the ℓ-th eigenvector and the associated eigenvalue, solutions of the following eigenproblem:

$$\mathbf{K}_i \boldsymbol{\psi}_i^{(\ell)} = \lambda_i^{(\ell)} \mathbf{K}_0 \boldsymbol{\psi}_i^{(\ell)}, \qquad (i = 1,\ldots,r;\ \ell = 1,\ldots,p_i). \tag{22}$$

The eigenvalues $\lambda_i^{(\ell)}$ are real positive numbers. Furthermore, the eigenvectors $\boldsymbol{\psi}_i^{(\ell)}$ are assumed to satisfy the orthonormalization condition:

$$\boldsymbol{\Psi}_i^{\mathrm{T}} \mathbf{K}_0 \boldsymbol{\Psi}_i = \mathbf{I}_{p_i}; \quad \boldsymbol{\Psi}_i = \left[\boldsymbol{\psi}_i^{(1)} \quad \boldsymbol{\psi}_i^{(2)} \quad \cdots \quad \boldsymbol{\psi}_i^{(p_i)} \right], \tag{23}$$

so that the following relationship holds:

$$\boldsymbol{\Psi}_i^{\mathrm{T}} \mathbf{K}_i \boldsymbol{\Psi}_i = \boldsymbol{\Lambda}_i; \quad \boldsymbol{\Lambda}_i = \mathrm{Diag}\left[\lambda_i^{(1)}, \quad \lambda_i^{(2)}, \quad \ldots \quad \lambda_i^{(p_i)} \right]. \tag{24}$$

Notice that only $p_i < n$ eigenvalues are different from zero and the generic term $\lambda_i^{(\ell)}\mathbf{v}_i^{(\ell)}\mathbf{v}_i^{(\ell)\mathrm{T}}$ of the summation in Eq. (20) turns out to be a rank-one matrix.

Substituting Eq. (20) into Eq. (18), the interval stiffness matrix can be rewritten in the following form:

$$\mathbf{K}^I = \mathbf{K}_0 + \sum_{i=1}^{r}\sum_{\ell=1}^{p_i}\lambda_i^{(\ell)}\mathbf{v}_i^{(\ell)}\mathbf{v}_i^{(\ell)\mathrm{T}}\Delta\alpha_i\,\hat{e}_i^I \tag{25}$$

where the deviation with respect to the nominal value is expressed as superposition of $r \times p_i$ matrices of rank one. Then, by applying the *IRSE* truncated to first-order terms [31, 34-36], the following approximate explicit expression of the inverse of the interval stiffness matrix is obtained:

$$\left(\mathbf{K}^I\right)^{-1} \approx \mathbf{K}_0^{-1} - \sum_{i=1}^{r}\sum_{\ell=1}^{p_i}\frac{\lambda_i^{(\ell)}\Delta\alpha_i\,\hat{e}_i^I}{1+\lambda_i^{(\ell)}d_{i\ell}\,\Delta\alpha_i\,\hat{e}_i^I}\mathbf{D}_{i\ell} = \mathbf{K}_0^{-1} + \sum_{i=1}^{r}\sum_{\ell=1}^{p_i}\left(\tilde{a}_{0,i\ell} + \Delta\tilde{a}_{0,i\ell}\hat{e}_i^I\right)\mathbf{D}_{i\ell} \tag{26}$$

where

$$d_{i\ell} = \mathbf{v}_i^{(\ell)\mathrm{T}}\mathbf{K}_0^{-1}\mathbf{v}_i^{(\ell)}; \quad \mathbf{D}_{i\ell} = \mathbf{K}_0^{-1}\mathbf{v}_i^{(\ell)}\mathbf{v}_i^{(\ell)\mathrm{T}}\mathbf{K}_0^{-1} \tag{27a,b}$$

and

$$\tilde{a}_{0,i\ell} = \frac{\left(\lambda_i^{(\ell)}\Delta\alpha_i\right)^2 d_{i\ell}}{1-\left(\lambda_i^{(\ell)}\Delta\alpha_i d_{i\ell}\right)^2}; \qquad \Delta\tilde{a}_{0,i\ell} = \frac{\lambda_i^{(\ell)}\Delta\alpha_i}{1-\left(\lambda_i^{(\ell)}\Delta\alpha_i d_{i\ell}\right)^2} \tag{28a,b}$$

denote the midpoint and deviation amplitude of the generic series term rewritten in affine form. In Eqs. (28a,b), the argument $\Delta\alpha_i$ of the functions $\tilde{a}_{0,i\ell}$ and $\Delta\tilde{a}_{i\ell}$ is omitted for conciseness.

Equation (26) may be viewed as the extension of the series expansion derived in [43] for structures with interval axial stiffness. It is worth mentioning that Eq. (26) holds if and only if the conditions $\left|\Delta\alpha_i\, d_i\right| < 1$ are satisfied. Obviously, the accuracy of Eq. (26) depends on the magnitude of the fluctuations $\Delta\alpha_i$. To handle large uncertainties satisfying the restriction $\Delta\alpha_i < 1$, in general, higher-order terms need to be retained in the *IRSE*.

The main advantage of the decomposition (25) of the interval stiffness matrix $\mathbf{K}^I$ with respect to the one adopted by the authors in their previous works [31, 35-36] lies in the small number $p_i < n$ of non-zero eigenvalues $\lambda_i^{(\ell)}$ of the matrix pair $(\mathbf{K}_i, \mathbf{K}_0)$. It can be readily verified that such number corresponds to the number of the structural natural deformation modes influenced by the single interval parameter α_i^I [44] and, therefore, it depends on the type of finite element (FE) employed in the model. For instance, since a bar type FE is characterized by one deformation mode, only one eigenvalue is different from zero. For a beam type FE, characterized by two deformation modes, two non-zero eigenvalues are obtained as solution of the eigenproblem (22), and so on.

Upon replacing the *IRSE* (26) of the inverse of the interval stiffness matrix in Eq. (9) and applying the *improved interval analysis via EUI* [33], the following approximate explicit expressions of the *LB* and *UB* of the interval mean-value, μ_Y^I, can be readily obtained:

$$\underline{\mu}_Y(\boldsymbol{\alpha}) = \mathrm{mid}\left\{\mu_Y^I\right\} - \Delta\mu_Y(\boldsymbol{\alpha}); \quad \overline{\mu}_Y(\boldsymbol{\alpha}) = \mathrm{mid}\left\{\mu_Y^I\right\} + \Delta\mu_Y(\boldsymbol{\alpha}) \tag{29a,b}$$

where

$$\mathrm{mid}\left\{\mu_Y^I\right\} = \mathbf{q}^{\mathrm{T}}\left[\mathbf{K}_0^{-1} + \sum_{i=1}^{r}\sum_{\ell=1}^{p_i}\tilde{a}_{0,i\ell}\mathbf{D}_{i\ell}\right]\boldsymbol{\mu}_{\mathbf{f}}; \quad \Delta\mu_Y(\boldsymbol{\alpha}) = \sum_{i=1}^{r}\left|\sum_{\ell=1}^{p_i}\Delta\tilde{a}_{i\ell}\,\mathbf{q}^{\mathrm{T}}\mathbf{D}_{i\ell}\boldsymbol{\mu}_{\mathbf{f}}\right| \tag{30a,b}$$

are the midpoint and deviation amplitude of the interval mean-value of the response process $Y^I(t)$, respectively. The symbol $|\bullet|$ denotes absolute value component wise.

4.2 Interval Spectral Moments

Approximate expressions of the interval spectral moments $\lambda_{j,\tilde{Y}}^I \equiv \lambda_{j,Y}^I$ $(j = 0, 2)$ of the random response process $Y^I(t)$ (see Eq. (17)) along with their bounds can be obtained by applying the *IRSE* for the evaluation of the interval *FRF* (see Eq. (11)) matrix $\mathbf{H}^I(\omega)$ needed to evaluate the interval *PSD* function $G_{\tilde{Y}\tilde{Y}}^I(\omega) \equiv G_{YY}^I(\omega)$ according to Eq. (10). To this aim, taking into account the

decomposition (18) of the interval stiffness matrix and Eq. (20), the damping matrix (6) can be expressed in the following form:

$$\mathbf{C}^I = \mathbf{C}_0 + c_1 \sum_{i=1}^{r} \mathbf{K}_i \, \Delta\alpha_i \, \hat{e}_i^I = \mathbf{C}_0 + c_1 \sum_{i=1}^{r} \sum_{\ell=1}^{p_i} \lambda_i^{(\ell)} \mathbf{v}_i^{(\ell)} \mathbf{v}_i^{(\ell)\mathrm{T}} \Delta\alpha_i \, \hat{e}_i^I \tag{31a,b}$$

where $\mathbf{C}_0 = c_0 \mathbf{M}_0 + c_1 \mathbf{K}_0$ is the nominal damping matrix. Then, introducing the following complex interval matrix:

$$\mathbf{P}^I(\omega) = p(\omega) \sum_{i=1}^{r} \mathbf{K}_i \, \Delta\alpha_i \, \hat{e}_i^I = p(\omega) \sum_{i=1}^{r} \sum_{\ell=1}^{p_i} \lambda_i^{(\ell)} \mathbf{v}_i^{(\ell)} \mathbf{v}_i^{(\ell)\mathrm{T}} \Delta\alpha_i \, \hat{e}_i^I \tag{32}$$

with

$$p(\omega) = 1 + \mathrm{j}\omega \, c_1 \tag{33}$$

the interval *FRF* matrix can be rewritten as:

$$\mathbf{H}^I(\omega) = \left[\mathbf{H}_0^{-1}(\omega) + \mathbf{P}^I(\omega) \right]^{-1} = \left[\mathbf{I}_n + \mathbf{H}_0(\omega) \mathbf{P}^I(\omega) \right]^{-1} \mathbf{H}_0(\omega). \tag{34}$$

In the previous equation, $\mathbf{I}_n$ denotes the identity matrix of order *n*; $\mathbf{H}_0(\omega)$ is the nominal *FRF* matrix, say for $\boldsymbol{\alpha} = \mathbf{0}$. Under the assumption of classically damped nominal structural system, the *FRF* matrix $\mathbf{H}_0(\omega)$ can be conveniently evaluated as:

$$\mathbf{H}_0(\omega) = \boldsymbol{\Phi}_0 \, \mathbf{H}_{0,\mathrm{m}}(\omega) \boldsymbol{\Phi}_0^{\mathrm{T}} \tag{35}$$

where $\boldsymbol{\Phi}_0$ is the nominal modal matrix of order $n \times s$ ($s \le n$) collecting the first s eigenvectors normalized with respect to the mass matrix $\mathbf{M}_0$. The matrix $\boldsymbol{\Phi}_0$ is obtained as solution of the following eigenproblem:

$$\mathbf{K}_0 \boldsymbol{\Phi}_0 = \mathbf{M}_0 \, \boldsymbol{\Phi}_0 \, \boldsymbol{\Omega}_0^2 ; \quad \boldsymbol{\Phi}_0^{\mathrm{T}} \mathbf{M}_0 \boldsymbol{\Phi}_0 = \mathbf{I}_s \tag{36a,b}$$

where $\boldsymbol{\Omega}_0^2 = \boldsymbol{\Phi}_0^{\mathrm{T}} \mathbf{K}_0 \boldsymbol{\Phi}_0$ is the spectral matrix of the nominal structural system, say a diagonal matrix listing the squares of the natural circular frequencies of the structure for the nominal values of the uncertain parameters. Furthermore, in Eq. (35) $\mathbf{H}_{0,\mathrm{m}}(\omega)$ denotes the modal transfer function matrix of the nominal structure that is a diagonal matrix given by:

$$\mathbf{H}_{0,\mathrm{m}}(\omega) = \left[-\omega^2 \mathbf{I}_s + \mathrm{j}\omega \boldsymbol{\Xi}_0 + \boldsymbol{\Omega}_0^2 \right]^{-1} \tag{37}$$

where $\boldsymbol{\Xi}_0 = c_0 \mathbf{I}_s + c_1 \boldsymbol{\Omega}_0$ is the generalised damping matrix.

By inspection of Eqs. (32) and (34), it is observed that the evaluation of the *FRF* matrix involves the inversion of a matrix expressed as sum of the nominal value plus a deviation given as superposition of rank-one matrices. It follows that the interval *FRF* matrix can be determined in approximate explicit form by applying the *IRSE* [31, 34-36], herein truncated to first-order terms, i.e.:

$$\mathbf{H}^I(\omega) \approx \mathbf{H}_0(\omega) - \sum_{i=1}^{r} \sum_{\ell=1}^{p_i} \frac{p(\omega) \lambda_i^{(\ell)} \Delta\alpha_i \, \hat{e}_i^I}{1 + p(\omega) \Delta\alpha_i \, \hat{e}_i^I \lambda_i^{(\ell)} \, b_{i\ell}(\omega)} \mathbf{B}_{i\ell}(\omega) = \mathbf{H}_{\mathrm{mid}}(\omega) + \mathbf{H}_{\mathrm{dev}}^I(\omega) \tag{38}$$

with

$$b_{i\ell}(\omega) = \mathbf{v}_i^{(\ell)\mathrm{T}} \mathbf{H}_0(\omega) \, \mathbf{v}_i^{(\ell)}; \quad \mathbf{B}_{i\ell}(\omega) = \mathbf{H}_0(\omega) \, \mathbf{v}_i^{(\ell)} \mathbf{v}_i^{(\ell)\mathrm{T}} \mathbf{H}_0(\omega). \tag{39a,b}$$

The *IRSE* in Eq. (38) holds if and only if the conditions $\left\| p(\omega) \Delta\alpha_i \, \lambda_i^{(\ell)} \, b_{i\ell}(\omega) \right\| < 1$ are satisfied, where the symbol $\|\bullet\|$ means modulus of $\bullet$.

According to the *improved interval analysis via EUI*, Eq. (38) provides the interval *FRF* matrix as sum of the midpoint, $\mathbf{H}_{\mathrm{mid}}(\omega)$, plus the interval deviation, $\mathbf{H}_{\mathrm{dev}}^I(\omega)$, given, respectively, by:

$$\begin{aligned} &\mathbf{H}_{\mathrm{mid}}(\boldsymbol{\alpha}, \omega) = \mathrm{mid}\left\{ \mathbf{H}^I(\omega) \right\} = \mathbf{H}_0(\omega) + \sum_{i=1}^{r} \sum_{\ell=1}^{p_i} a_{0,i\ell}(\omega) \mathbf{B}_{i\ell}(\omega); \\ &\mathbf{H}_{\mathrm{dev}}^I(\omega) = \mathrm{dev}\left\{ \mathbf{H}^I(\omega) \right\} = \sum_{i=1}^{r} \sum_{\ell=1}^{p_i} \Delta a_{i\ell}(\omega) \mathbf{B}_{i\ell}(\omega) \hat{e}_i^I = \sum_{i=1}^{r} \mathbf{R}_i(\omega) \hat{e}_i^I \end{aligned} \tag{40a,b}$$

where $\text{dev}\{\bullet\}$ denotes the interval deviation of the quantity between curly brackets. Furthermore, in Eqs. (40a,b)

$$\mathbf{R}_i(\omega) = \sum_{\ell=1}^{p_i} \Delta a_{i\ell}(\omega)\, \mathbf{B}_{i\ell}(\omega) \tag{41}$$

and

$$a_{0,i\ell}(\omega) = \frac{\left[\, p(\omega)\lambda_i^{(\ell)}\Delta\alpha_i \,\right]^2 b_{i\ell}(\omega)}{1-\left[\, p(\omega)\lambda_i^{(\ell)}\Delta\alpha_i\, b_{i\ell}(\omega)\right]^2};\quad \Delta a_{i\ell}(\omega) = \frac{p(\omega)\lambda_i^{(\ell)}\Delta\alpha_i}{1-\left[\, p(\omega)\lambda_i^{(\ell)}\Delta\alpha_i\, b_{i\ell}(\omega)\right]^2} \tag{42a,b}$$

where the argument $\Delta\alpha_i$ of the functions $a_{0,i\ell}(\omega)$ and $\Delta a_{i\ell}(\omega)$ is omitted for the sake of conciseness.

Upon substitution of the approximate interval *FRF* matrix (38) into Eq. (10), the interval *PSD* function of the random process $Y^I(t)$ can be expressed as sum of the midpoint value plus the interval deviation as well, i.e.:

$$G_{YY}(\boldsymbol{\alpha},\omega) = \text{mid}\left\{G_{YY}(\boldsymbol{\alpha},\omega)\right\} + \text{dev}\left\{\hat{G}_{YY}(\boldsymbol{\alpha},\omega)\right\},\quad \boldsymbol{\alpha}\in\boldsymbol{\alpha}^I = \left[\underline{\boldsymbol{\alpha}},\overline{\boldsymbol{\alpha}}\right] \tag{43}$$

where

$$\begin{aligned}
&\text{mid}\left\{G_{YY}^I(\omega)\right\} = \mathbf{q}^{\mathrm{T}}\mathbf{H}_{\text{mid}}^{*}(\boldsymbol{\alpha},\omega)\,\mathbf{G}_{\tilde{\mathbf{X}}_\mathbf{f}\tilde{\mathbf{X}}_\mathbf{f}}(\omega)\,\mathbf{H}_{\text{mid}}^{\mathrm{T}}(\boldsymbol{\alpha},\omega)\mathbf{q};\\
&\text{dev}\left\{\hat{G}_{YY}^I(\omega)\right\} = \sum_{i=1}^{r}\mathbf{q}^{\mathrm{T}}\left[\mathbf{H}_{\text{mid}}^{*}(\boldsymbol{\alpha},\omega)\,\mathbf{G}_{\tilde{\mathbf{X}}_\mathbf{f}\tilde{\mathbf{X}}_\mathbf{f}}(\omega)\mathbf{R}_i^{\mathrm{T}}(\omega) + \mathbf{R}_i^{*}(\omega)\mathbf{G}_{\tilde{\mathbf{X}}_\mathbf{f}\tilde{\mathbf{X}}_\mathbf{f}}(\omega)\,\mathbf{H}_{\text{mid}}^{\mathrm{T}}(\boldsymbol{\alpha},\omega)\right]\mathbf{q}\,\hat{e}_i^I.
\end{aligned} \tag{44a,b}$$

The over hat in Eq. (44b) means that an approximate expression of the deviation matrix is assumed. Specifically, in order to simplify interval computations, terms associated with powers of $\Delta\alpha_i$ greater than one are neglected [34].

Finally, taking into account Eq. (43), the interval spectral moments (17) can be recast in the following form:

$$\lambda_{j,\tilde{Y}}(\boldsymbol{\alpha}) = \lambda_{j,Y}(\boldsymbol{\alpha}) = \mathrm{mid}\left\{\lambda_{j,Y}(\boldsymbol{\alpha})\right\} + \mathrm{dev}\left\{\hat{\lambda}_{j,Y}(\boldsymbol{\alpha})\right\}, \quad \boldsymbol{\alpha} \in \boldsymbol{\alpha}^I = \left[\underline{\boldsymbol{\alpha}}, \overline{\boldsymbol{\alpha}}\right]; \;\; j = 0, 2 \tag{45}$$

where

$$\mathrm{mid}\left\{\lambda_{j,Y}(\boldsymbol{\alpha})\right\} = 2\int_0^\infty \omega^j \mathrm{mid}\left\{G_{YY}(\boldsymbol{\alpha}, \omega)\right\} \mathrm{d}\omega; \quad \mathrm{dev}\left\{\hat{\lambda}_{j,Y}(\boldsymbol{\alpha})\right\} = 2\int_0^\infty \omega^j \mathrm{dev}\left\{\hat{G}_{YY}(\boldsymbol{\alpha}, \omega)\right\} \mathrm{d}\omega. \tag{46a,b}$$

Based on Eq. (45), the *LB* and *UB* of the interval spectral moments can be evaluated in approximate form as:

$$\underline{\lambda}_{j,Y}(\boldsymbol{\alpha}) = \mathrm{mid}\left\{\lambda_{j,Y}^I\right\} - \Delta\lambda_{j,Y}(\boldsymbol{\alpha}); \qquad \overline{\lambda}_{j,Y}(\boldsymbol{\alpha}) = \mathrm{mid}\left\{\lambda_{j,Y}^I\right\} + \Delta\lambda_{j,Y}(\boldsymbol{\alpha}), \;\; j = 0, 2 \tag{47a,b}$$

where

$$\Delta\lambda_{j,Y}(\boldsymbol{\alpha}) = 2\sum_{i=1}^{r} \left| \int_0^\infty \omega^j \mathbf{q}^{\mathrm{T}} \left[\mathbf{H}_{\mathrm{mid}}^*(\boldsymbol{\alpha}, \omega) \mathbf{G}_{\tilde{\mathbf{X}}_{\mathrm{f}} \tilde{\mathbf{X}}_{\mathrm{f}}}(\omega) \mathbf{R}_i^{\mathrm{T}}(\omega) + \mathbf{R}_i^*(\omega) \mathbf{G}_{\tilde{\mathbf{X}}_{\mathrm{f}} \tilde{\mathbf{X}}_{\mathrm{f}}}(\omega) \mathbf{H}_{\mathrm{mid}}^{\mathrm{T}}(\boldsymbol{\alpha}, \omega) \right] \mathbf{q} \, \mathrm{d}\omega \right| \tag{48}$$

denotes the deviation amplitude.

Since the mean-value and the spectral moments of the response are monotonic functions of the generic uncertain parameter α_i^I, their exact bounds can be evaluated by applying the *vertex method*. As already mentioned, such combinatorial procedure is time consuming and becomes soon unfeasible as the number of uncertainties increases. Indeed, it requires 2^r stochastic analyses of the structure to compute response statistics corresponding to all possible combinations of the endpoints of the r interval parameters α_i^I. Conversely, the above described approach allows to handle an arbitrary number of uncertain parameters since it evaluates the bounds of the interval mean-value and spectral moments by handy formulas without resorting to any combinatorial procedure. Besides using the spectral decomposition of the interval stiffness matrix (see Eq.(25)), the computational efficiency of the proposed procedure can also be enhanced by performing a preliminary sensitivity analysis, as recently outlined by the authors [31]. Indeed, sensitivity analysis allows to detect the

least influential uncertain parameters and then neglect the associated contributions in the approximate expression of the response quantity bounds provided by the *IRSE*.

5 BOUNDS OF THE INTERVAL RELIABILITY FUNCTION

Structural design, in general, consists of proportioning the elements of a structure such that it satisfies various criteria of safety, serviceability and durability under the action of loads. In other words, the structure should be designed such that it has a higher strength or resistance than the effects caused by loads. In the framework of structural design, the reliability of a structural system is its ability to fulfill its design purpose for some specified reference period and its efficient estimation is a crucial issue for problems with uncertainties.

Within the interval framework, the aim of reliability analysis is to determine the range of structural performance. Specifically, for the selected *extreme value* random process, $Y_{\max}^{I}(T)$, the *LB* and *UB* of the *interval reliability function*, $L_{Y_{\max}}^{I}(b,T)$, need to be evaluated (see Eq. (14)).

Since the interval *CDF*, $L_{Y_{\max}}^{I}(b,T)$, is a monotonic function of the generic uncertain parameter α_i^I, its exact bounds can be determined by applying the *vertex method* (see e.g., [28]). The latter is a combinatorial procedure which requires to evaluate the *reliability function* of the selected *extreme value* process, $Y_{\max}^{I}(T)$, for all the combinations of the bounds of the r uncertain parameters α_i^I, say 2^r, and then take, for a fixed barrier level *b*, the maximum and minimum value among all the *CDFs* so obtained. Obviously, the *vertex method* becomes prohibitive for real-sized structures involving a large number of uncertainties. Indeed, each evaluation of the *CDF* implies an onerous stochastic analysis of the structure in order to compute the mean-value and spectral moments of the response pertaining to a specific combination of the bounds of the uncertain parameters. Recently, the authors proposed an approximate procedure for the evaluation of the interval *CDF* bounds based on *first-order interval Taylor series expansion* [31]. Such procedure is more efficient from a

computational point of view than the *vertex method*, but its accuracy worsens as large uncertainty levels are involved.

To overcome this limitation, in the present paper a novel approach based on the philosophy of the *vertex method* is proposed for determining the interval reliability region. The key idea is to view the *interval reliability function*, $L^I_{Y_{\max}}(b,T)$, herein rewritten for the sake of clarity

$$L^I_{Y_{\max}}(b,T) \approx \exp\left[-\frac{T}{2\pi}\sqrt{\frac{\lambda^I_{2,Y}}{\lambda^I_{0,Y}}}\exp\left(-\frac{(b-\mu^I_Y)^2}{2\lambda^I_{0,Y}}\right)\right] \equiv L^I_{Y_{\max}}\left(b,T;\mu^I_Y,\lambda^I_{0,Y},\lambda^I_{2,Y}\right) \tag{49}$$

as function of three interval parameters μ^I_Y, $\lambda^I_{0,Y}$ and $\lambda^I_{2,Y}$, say the interval mean-value and spectral moments of order $j=0,2$, rather than as depending on the r uncertain parameters α^I_i. This provides substantial computational savings since the bounds of the interval *CDF* can be evaluated by a combinatorial approach performing only 2^3 evaluations of the *CDF* corresponding to all possible combinations of the bounds of the three intervals μ^I_Y, $\lambda^I_{0,Y}$ and $\lambda^I_{2,Y}$ defined in approximate form by Eqs. (29a,b) and (47a,b). A deeper insight into Eq. (49) allows to further reduce the number of *CDF* evaluations required by the combinatorial approach. Indeed, it can be readily inferred that in order to estimate the *LB* of the *interval reliability function*, $\underline{L}_{Y_{\max}}(b,T)$, the interval mean-value and the second-order spectral moment have to be set to their *UB*, $\overline{\mu}_Y$ and $\overline{\lambda}_{2,Y}$, respectively. Conversely, the evaluation of the *UB* of the interval *CDF*, $\overline{L}_{Y_{\max}}(b,T)$, requires to set the interval mean-value and second-order spectral moment at their *LB*, $\underline{\mu}_Y$ and $\underline{\lambda}_{2,Y}$. Based on these observations, the bounds of the *interval reliability function*, $L^I_{Y_{\max}}(b,T)$, can be expressed as follows:

$$\underline{L}_{Y_{\max}}(b,T)=\min_{\lambda_{0,Y}\in\lambda_{0,Y}^{I}} L_{Y_{\max}}\left(b,T;\overline{\mu}_{Y},\lambda_{0,Y}^{I},\overline{\lambda}_{2,Y}\right)=\min_{\lambda_{0,Y}\in\lambda_{0,Y}^{I}}\left\{\exp\left[-\frac{T}{2\pi}\sqrt{\frac{\overline{\lambda}_{2,Y}}{\lambda_{0,Y}^{I}}}\exp\left(-\frac{(b-\overline{\mu}_{Y})^{2}}{2\lambda_{0,Y}^{I}}\right)\right]\right\};$$
$$\overline{L}_{Y_{\max}}(b,T)=\max_{\lambda_{0,Y}\in\lambda_{0,Y}^{I}} L_{Y_{\max}}\left(b,T;\underline{\mu}_{Y},\lambda_{0,Y}^{I},\underline{\lambda}_{2,Y}\right)=\max_{\lambda_{0,Y}\in\lambda_{0,Y}^{I}}\left\{\exp\left[-\frac{T}{2\pi}\sqrt{\frac{\underline{\lambda}_{2,Y}}{\lambda_{0,Y}^{I}}}\exp\left(-\frac{(b-\underline{\mu}_{Y})^{2}}{2\lambda_{0,Y}^{I}}\right)\right]\right\} \quad (50a,b)$$

where the symbols $\min\{\bullet\}$ and $\max\{\bullet\}$ mean minimum and maximum value of the quantity into curly parentheses, respectively. Such quantity is an interval function which turns out to depend on just one interval parameter, say $\lambda_{0,Y}^{I}=\left[\underline{\lambda}_{0,Y},\overline{\lambda}_{0,Y}\right]$. Hence, for each barrier level b, the *LB* and *UB* of the *interval reliability function* $L_{Y_{\max}}^{I}(b,T)$ can be readily obtained as the minimum and maximum among the *CDFs* pertaining to the bounds of the zero-order interval spectral moment of the response $\lambda_{0,Y}^{I}=\left[\underline{\lambda}_{0,Y},\overline{\lambda}_{0,Y}\right]$ when the interval mean-value and second-order spectral moment are set at their upper or lower bounds, respectively, as indicated in Eqs. (50a,b), i.e.:

$$\underline{L}_{Y_{\max}}(b,T)=\min\left\{L_{Y_{\max}}^{(1)},L_{Y_{\max}}^{(2)}\right\};\quad \overline{L}_{Y_{\max}}(b,T)=\max\left\{L_{Y_{\max}}^{(3)},L_{Y_{\max}}^{(4)}\right\} \quad (51a,b)$$

where

$$L_{Y_{\max}}^{(1)}=L_{Y_{\max}}\left(b,T;\overline{\mu}_{Y},\underline{\lambda}_{0,Y},\overline{\lambda}_{2,Y}\right);\quad L_{Y_{\max}}^{(2)}=L_{Y_{\max}}\left(b,T;\overline{\mu}_{Y},\overline{\lambda}_{0,Y},\overline{\lambda}_{2,Y}\right);$$
$$L_{Y_{\max}}^{(3)}=L_{Y_{\max}}\left(b,T;\underline{\mu}_{Y},\underline{\lambda}_{0,Y},\underline{\lambda}_{2,Y}\right);\quad L_{Y_{\max}}^{(4)}=L_{Y_{\max}}\left(b,T;\underline{\mu}_{Y},\overline{\lambda}_{0,Y},\underline{\lambda}_{2,Y}\right). \quad (52a\text{-}d)$$

The main steps of the presented procedure may be summarized as follows: *i*) to perform the spectral decomposition of the interval stiffness matrix (see Eq. (25)); *ii*) to evaluate the inverse of the interval stiffness matrix (Eq. (26)) and the associated *FRF* matrix (Eq. (38)) in approximate explicit form by applying the *IRSE*; *iii*) to derive approximate expressions of the bounds of the interval mean-value (Eqs. (29a,b)) and zero- and second-order spectral moments (Eqs. (47a,b)) of the selected response process; *iv*) to determine the range of the *interval reliability function* by exploring four combinations of the bounds of response statistics computed in the previous step, two for the *LB* (see Eq. (51a)) and two for the *UB* of the interval *CDF* (see Eq. (51b)).

It is worth emphasizing that the described procedure overall requires to explore only four combinations of the interval mean-value and spectral moments of the response, regardless of the number of uncertain structural parameters involved. Conversely, the computational effort of the *vertex method* increases with the number of uncertainties. Furthermore, each evaluation of the *CDF* does not require a new stochastic analysis of the structure, but involves the computed bounds of the mean-value and spectral moments of the response.

6 NUMERICAL APPLICATIONS

As pointed out in the previous sections, aim of this study is to provide a procedure able to evaluate approximate bounds of structural system reliability or probability of failure in the presence of stochastic excitations and unavoidable uncertainties modeled as interval parameters.

The presented procedure has been implemented into a computer algorithm employed to provide the reliability bounds. Due to its simplicity and effectiveness, the algorithm allows to obtain very accurate results for the bounds of the reliability function avoiding the high computational effort and the related time consuming operations required by the *vertex method* which become increasingly substantial with larger number of interval variables. The details of the algorithm and its implementation are presented in the flow-chart reported in Fig. 1.

The algorithm is used in two structural examples -a steel 25-bar truss structure and a steel chimney structure- with varying levels of uncertainty of Young's modulus and subjected to turbulent wind loads in the *x* -direction.

The nodal forces $F_{x,i}(z_i,t)$ modelling the wind excitation are functions of the height *z* and time *t* expressed in terms of the mean, $F_{x,i}^{(s)}(z_i)$, and random, $\tilde{F}_{x,i}(z_i,t)$, components of wind loads as follows [45]:

$$F_{x,i}(z_i,t) = F_{x,i}^{(s)}(z_i) + \tilde{F}_{x,i}(z_i,t) \tag{53}$$

where $F_{x,i}^{(s)}(z_i) \approx \rho C_D A_i w_s^2(z_i)/2$ and $\tilde{F}_{x,i}(z_i,t) \approx \rho C_D A_i \tilde{W}(z_i,t) w_s(z_i)$ are related, respectively, to the mean-value, $w_s(z)$, and the fluctuating component, $\tilde{W}(z,t)$, of the wind velocity field $W(z,t) = w_s(z) + \tilde{W}(z,t)$. The parameters ρ, C_D and A_i involved in the expressions of $F_{x,i}^{(s)}(z_i)$ and $\tilde{F}_{x,i}(z_i,t)$ are the air density, the drag coefficient and the tributary area of the i-th node, respectively. For both numerical applications, ρ and C_D are selected as follows: $\rho = 1.25$ kg/m^3 and $C_D = 1.2$. For the mean wind velocity, a power law variation with the elevation z is assumed, that is $w_s(z) = w_{s,10}\left(z/10\right)^{\gamma}$, where $w_{s,10}$ is the mean wind speed measured at height $z = 10$ m above ground and γ is a coefficient depending on surface roughness, herein taken equal to $w_{s,10} = 25$ m/s and $\gamma = 0.3$, respectively.

The fluctuating components due to the turbulence in the flowing wind are correlated and modelled as zero-mean stationary Gaussian random processes fully described from a probabilistic point of view by the cross-*PSD* functions $G_{\tilde{W}_i\tilde{W}_j}(z_i, z_j; \omega) = G_{\tilde{W}\tilde{W}}(\omega)\, f_{ij}(\omega)$ with:

$$G_{\tilde{W}\tilde{W}}(\omega) = 4K_0 w_{s,10}^2 \frac{\chi^2}{\omega\left(1+\chi^2\right)^{4/3}}; \quad f_{ij}(\omega) = \exp\left\{-\frac{|\omega|\sqrt{C_z^2(z_i - z_j)^2}}{\pi\left[w_s(z_i) + w_s(z_j)\right]}\right\} \tag{54a,b}$$

where $G_{\tilde{W}\tilde{W}}(\omega)$ is the two-sided Davenport's power spectrum [46] and $f_{ij}(\omega)$ is the so-called coherence function. The parameter K_0 is the non-dimensional roughness coefficient, herein set equal to $K_0 = 0.03$, and $\chi = b_1\omega/(\pi v_{s,10})$ with $b_1 = 600$ m; C_z denotes an appropriate decay coefficient to be determined experimentally, herein set equal to $C_z = 10$.

6.1 Wind-Excited Truss Structure

The first numerical application concerns a 25-bar truss structure, as shown in Fig. 2. Lengths and cross-sectional areas of the bars are supposed to be deterministic: all the bars are assumed to have

cross-sectional area $A_{0,i} = A_0 = 7 \times 10^{-4} \mathrm{m}^2$ $(i = 1,2,\ldots,25)$ and lengths $L_{0,i}$ $(i = 1,2,\ldots,25)$ inferable from Fig. 2 where $L = 5.1 \mathrm{m}$. Furthermore, each node possesses a lumped mass $M = 500 \mathrm{kg}$. Young's moduli of the diagonal bars are modeled as interval parameters $E_i^I = E_0 \left(1 + \Delta\alpha_i \hat{e}_i^I\right)$, $(i = 16,17,...,25)$ with midpoint value $E_0 = 2.1 \times 10^8 \, \mathrm{kN/m}^2$ and deviation amplitudes $\Delta\alpha_i = \Delta\alpha$ satisfying the condition $\Delta\alpha < 1$.

The Rayleigh damping constants $c_0 = 1.123836 \, s^{-1}$ and $c_1 = 0.001126 \, s$ (see Eq. (6)) are evaluated in such a way that the modal damping ratio for the first and third modes of the nominal structure is $\zeta_0 = 0.05$.

The horizontal and vertical displacement random processes of the *j*-th node are denoted by $U_j(\boldsymbol{\alpha}^I, t) = \mu_{U_j}(\boldsymbol{\alpha}^I) + \tilde{U}_j(\boldsymbol{\alpha}^I, t)$ and $V_j(\boldsymbol{\alpha}^I, t) = \mu_{V_j}(\boldsymbol{\alpha}^I) + \tilde{V}_j(\boldsymbol{\alpha}^I, t)$, respectively.

As previously outlined, the truss structure is subjected to nodal forces $F_{x,i}(z_i, t)$ (see Eq. (53)) in the along-wind direction applied to nodes 1,3,5,7 and 9 (see Fig. 2) located at different heights $z_i = i\,L_i$ $(i = 1,3,5,7,9)$. The tributary areas appearing in the expressions of the mean and fluctuating components of the nodal forces have values $A_1 = A_3 = A_5 = A_7 = 26.01 \, \mathrm{m}^2$ and $A_9 = 13.005 \, \mathrm{m}^2$, respectively.

In the spectral decomposition of the matrix $\mathbf{K}_i$ pertaining to the truss structure, only one eigenvalue (solution of the eigenproblem reported in Eq. (22)) is different from zero, i.e. $p_i = 1$, which leads to the expression $\mathbf{K}_i = \lambda_i \mathbf{v}_i \mathbf{v}_i^{\mathrm{T}}$ for the rank-one matrices defined in Eq. (20). The latter observation yields a substantial reduction of the computational effort since only the summation over the uncertain parameters needs to be considered in Eq. (25).

The attention is focused on the interval *extreme value* stochastic processes of the horizontal displacements of nodes 1 and 9, say $Y_{\max}^I(T) = U_{1\max}^I(T)$ and $Y_{\max}^I(T) = U_{9\max}^I(T)$, and the bounds of

the related *interval reliability functions*, $L^I_{U_{1\max}}(b,T)$ and $L^I_{U_{9\max}}(b,T)$, are evaluated for two levels of uncertainty $\Delta\alpha$, namely $\Delta\alpha = 0.1$ and $\Delta\alpha = 0.15$. The time interval T is selected as $T = 1000\ T_0$, T_0 being the fundamental period of the truss structure.

As outlined in Section 5, the evaluation of the *LB* and *UB* of the *extreme value CDF* (see Eq. (49)) follows the proposed combinatorial approach which involves the bounds of the interval mean-value (see Eq. (29a,b)) and zero- and second-order spectral moments (see Eq. (47a,b)). In particular, the proposed procedure requires only 2 combinations of the bounds of the zero-order spectral moment in order to evaluate each bound of the *reliability function* of the selected *extreme value* random process (see Eqs. (51a,b)), whatever the number of uncertainties is. On the other hand, it has to be emphasized that application of the *vertex method* to evaluate the exact bounds of the *extreme value CDF* requires $2^r = 2^{10}$ stochastic analyses for the case under exam.

In Figs. 3 and 4, the estimates of the *LB* and *UB* of the *interval reliability functions* $L^I_{U_{1\max}}(b,T)$ and $L^I_{U_{9\max}}(b,T)$ provided by the proposed procedure are contrasted with the exact bounds. For the sake of completeness, the nominal reliability functions, $L^{(0)}_{U_{1\max}}(b,T)$ and $L^{(0)}_{U_{9\max}}(b,T)$, are also plotted. It is worth noting that for $\Delta\alpha = 0.1$ (see Figs. 3a), the *UB* and *LB* of $L^I_{U_{1\max}}(b,T)$ provided by the proposed approach are almost coincident with the exact ones. Furthermore, as shown in Fig. 3b, an excellent agreement between the proposed and exact bounds of $L^I_{U_{1\max}}(b,T)$ is also obtained for larger deviation amplitudes of the interval Young's moduli, say $\Delta\alpha = 0.15$. Very accurate estimates of the bounds of the *CDF* of the horizontal displacement of node 9 of the truss structure, $L^I_{U_{9\max}}(b,T)$, are obtained for both levels of uncertainty, namely $\Delta\alpha = 0.1$ and $\Delta\alpha = 0.15$, as shown in the comparison between the exact and proposed *UB* and *LB* depicted in Fig. 4. As expected, the region of the *interval reliability function* becomes wider as the uncertainty level increases. Furthermore, comparison between the regions of the interval *CDFs*, $L^I_{U_{1\max}}(b,T)$ and $L^I_{U_{9\max}}(b,T)$,

shows that reliability assessment in terms of the *extreme value* stochastic process $Y^I_{\max}(T) = U^I_{1\max}(T)$ is much more affected by uncertainty of Young's moduli. Obviously, only the *LB* of the *interval reliability function* is useful for design purpose, since the *UB* may overestimate the actual performance of the structure in operating conditions.

Other quantities of interest for the structural design -since strictly related to structural performance- are the interval mean-value $\mu^I_{Y_{\max}}(T)$ and interval variance $\sigma^{2\,I}_{Y_{\max}}(T)$ of the *extreme value* random process $Y^I_{\max}(T)$. Following the formulation proposed by Davenport [47] and applying interval extension, the approximate expressions for the interval mean-value, $\mu^I_{Y_{\max}}(T)$, and interval variance, $\sigma^{2\,I}_{Y_{\max}}(T)$, are provided, respectively, by:

$$\mu^I_{Y_{\max}}(T) \approx \left(\sqrt{2\ln\left(\nu^{+I}_Y T\right)} + \frac{0.5772}{\sqrt{2\ln\left(\nu^{+I}_Y T\right)}} \right) \sigma^I_Y \tag{55}$$

and

$$\sigma^{2\,I}_{Y_{\max}}(T) \approx \left(\frac{\pi^2}{12\ln\left(\nu^{+I}_Y T\right)} \right) \sigma^{2\,I}_Y \,. \tag{56}$$

It is worth observing that the previous relationships provide both $\mu^I_{Y_{\max}}(T)$ and $\sigma^I_{Y_{\max}}(T)$ as explicit expressions of zero- and second-order spectral moments of the response process $Y^I(t)$. Indeed, ν^{+I}_Y denotes the mean up-crossing rate at level $\mu^I_Y > 0$, defined in Eq. (16) in terms of $\lambda^I_{0,Y}$ and $\lambda^I_{2,Y}$, while $\sigma^{2\,I}_Y$ is the interval variance of $Y^I(t)$ which coincides with the zero-order interval spectral moment $\lambda^I_{0,Y}$.

Following the philosophy of the so-called *structural reliability index* introduced in engineering practice as a measure of structural safety, an interval index, labelled as $\beta^I_{Y_{\max}}(T)$, and related to the ratio of mean-value of $Y^I_{\max}(T)$ (see Eq. (55)) to its standard deviation (see Eq. (56)) is here

introduced in order to provide a further validation of the accuracy of the proposed procedure. In this context, the interval index, $\beta_{Y_{\max}}^{I}(T)$, is defined as follows:

$$\beta_{Y_{\max}}^{I}(T)=\left[\underline{\beta}_{Y_{\max}}(T),\overline{\beta}_{Y_{\max}}(T)\right]=\frac{b_0-\mu_{Y_{\max}}^{I}(T)}{\sigma_{Y_{\max}}^{I}(T)} \tag{57}$$

where b_0 is a deterministic critical level selected for the response variable b, while $\mu_{Y_{\max}}^{I}(T)=\left[\underline{\mu}_{Y_{\max}}(T),\overline{\mu}_{Y_{\max}}(T)\right]$ and $\sigma_{Y_{\max}}^{I}(T)=\left[\underline{\sigma}_{Y_{\max}}(T),\overline{\sigma}_{Y_{\max}}(T)\right]$ are the interval mean-value and interval standard deviation of $Y_{\max}^{I}(T)$, respectively, given by Eqs. (55) and (56).

By applying the rules of interval analysis to Eq. (57), the *LB* and *UB* of the interval index, $\beta_{Y_{\max}}^{I}(T)$, are straightforwardly obtained as:

$$\underline{\beta}_{Y_{\max}}(T)=\frac{b_0-\overline{\mu}_{Y_{\max}}(T)}{\overline{\sigma}_{Y_{\max}}(T)};\quad \overline{\beta}_{Y_{\max}}=\frac{b_0-\underline{\mu}_{Y_{\max}}(T)}{\underline{\sigma}_{Y_{\max}}(T)} \tag{58a,b}$$

and their evaluation requires the knowledge of the bounds of the interval mean-value and standard deviation of $Y_{\max}^{I}(T)$.

Taking into account the explicit expressions (55) and (56) of $\mu_{Y_{\max}}^{I}(T)$ and $\sigma_{Y_{\max}}^{I}(T)$ in terms of zero- and second-order spectral moments, their bounds can be obtained straightforwardly by applying the rules of interval analysis, i.e.:

$$\begin{aligned}
\underline{\mu}_{Y_{\max}}(T)&=\left(\sqrt{2\ln\left(\frac{T}{2\pi}\sqrt{\underline{\lambda}_{2,Y}(\boldsymbol{\alpha})/\underline{\lambda}_{0,Y}(\boldsymbol{\alpha})}\right)}+\frac{0.5772}{\sqrt{2\ln\left(\frac{T}{2\pi}\sqrt{\underline{\lambda}_{2,Y}(\boldsymbol{\alpha})/\underline{\lambda}_{0,Y}(\boldsymbol{\alpha})}\right)}}\right)\sqrt{\underline{\lambda}_{0,Y}(\boldsymbol{\alpha})};\\
\overline{\mu}_{Y_{\max}}(T)&=\left(\sqrt{2\ln\left(\frac{T}{2\pi}\sqrt{\overline{\lambda}_{2,Y}(\boldsymbol{\alpha})/\overline{\lambda}_{0,Y}(\boldsymbol{\alpha})}\right)}+\frac{0.5772}{\sqrt{2\ln\left(\frac{T}{2\pi}\sqrt{\overline{\lambda}_{2,Y}(\boldsymbol{\alpha})/\overline{\lambda}_{0,Y}(\boldsymbol{\alpha})}\right)}}\right)\sqrt{\overline{\lambda}_{0,Y}(\boldsymbol{\alpha})}
\end{aligned} \tag{59a,b}$$

and

$$\underline{\sigma}_{Y_{\max}}(T)=\left(\frac{\pi}{2\sqrt{3\ln\left(\frac{T}{2\,\pi}\sqrt{\bar{\lambda}_{2,Y}(\boldsymbol{\alpha})/\underline{\lambda}_{0,Y}(\boldsymbol{\alpha})}\right)}}\right)\sqrt{\underline{\lambda}_{0,Y}(\boldsymbol{\alpha})};$$

$$\bar{\sigma}_{Y_{\max}}(T)=\left(\frac{\pi}{2\sqrt{3\ln\left(\frac{T}{2\,\pi}\sqrt{\underline{\lambda}_{2,Y}(\boldsymbol{\alpha})/\bar{\lambda}_{0,Y}(\boldsymbol{\alpha})}\right)}}\right)\sqrt{\bar{\lambda}_{0,Y}(\boldsymbol{\alpha})}. \tag{60a,b}$$

The previous relationships involve the bounds of zero- and second-order spectral moments which can be evaluated by the proposed procedure as outlined in Section 4 (see Eqs. (29a,b) and (47a,b)).

Once the *LB* and *UB* of the interval mean-value and standard deviation, $\mu^I_{Y_{\max}}(T)$ and $\sigma^I_{Y_{\max}}(T)$, are determined as reported in Eqs. (59a,b) and (60a,b), the bounds of the interval index $\beta^I_{Y_{\max}}(T)$ for the selected random process $Y^I_{\max}(T)$ can be derived by applying Eqs. (58a,b).

The index bounds, $\underline{\beta}_{Y_{\max}}(T)$ and $\bar{\beta}_{Y_{\max}}(T)$, are here evaluated for the *extreme value* process $Y^I_{\max}(T)=U^I_{9\max}(T)$ of the horizontal displacement of node 9 of the truss structure considering four different values of the threshold b_0. The estimates of the bounds obtained following both the *vertex method* (exact values) and the proposed procedure are reported in Table 1. Table 1 also shows the absolute percentage error defined as:

$$\varepsilon_\beta(\%)=\frac{\left|\beta^{(exact)}_{Y\max}-\beta^{(proposed)}_{Y\max}\right|}{\beta^{(exact)}_{Y\max}}\times 100 \tag{61}$$

where $\beta_{Y\max}$ takes the lower or the upper bound value. Notice that the percentage error does not exceed the 0.12% value, as further proof of the accuracy of the proposed procedure.

In order to estimate the dispersion of the *interval reliability function* with respect to the midpoint value, the so-called *coefficient of interval uncertainty* (c.i.u.) is introduced:

$$\text{c.i.u.}\left[L^I_{Y_{\max}}(b,T)\right] = \frac{\Delta L_{Y\max}(b,T)}{\text{mid}\left\{L^I_{Y\max}(b,T)\right\}} = \frac{\overline{L}_{Y\max}(b,T) - \underline{L}_{Y\max}(b,T)}{\overline{L}_{Y\max}(b,T) + \underline{L}_{Y\max}(b,T)}. \tag{62}$$

It allows to quantify the propagation of the uncertain input parameters to system reliability. Indeed, the *coefficient of interval uncertainty* may be viewed as the non-probabilistic counterpart of the well-known *coefficient of variation*.

The c.i.u. (in percentage) of the *extreme value* process $Y^I_{\max}(T) = U^I_{9\max}(T)$ of the truss structure under study, is found to be about 0.27% for a threshold $b_0 = 0.58$ m and $\Delta\alpha = 0.1$, while values of the c.i.u. of about 0.12 %, 0.049% and 0.020% are obtained for different thresholds, say $b_0 = 0.60, 0.62$ and 0.64 m, respectively. Notice that the dispersion of the interval *CDF* around the midpoint value increases as smaller thresholds corresponding to lower safety levels are considered.

6.2 Wind-Excited Steel Chimney

As second numerical application, the steel chimney structure depicted in Fig. 5 is considered. The chimney has tubular cross-section with external diameter $d = 1.45$ m and thickness $s = 0.01$ m, and height $H = 25.5$ m; the mass distribution is supposed to be deterministic. The Rayleigh damping constants appearing in Eq. (6) are taken as $c_0 = 1.227256\, s^{-1}$ and $c_1 = 0.000967\, s$, respectively, in such a way that the modal damping ratio for the first and second modes of the nominal structure is $\zeta_0 = 0.05$.

The chimney is modeled as a slender clamped-free beam discretized by five Euler-type finite elements of equal length $L_i = 5.1$ m (i=1,2,...,5), with two degrees of freedom at each node, as reported in Fig. 5.

Also in this numerical application, Young's modulus of each element is modeled as an interval parameter $E^I_i = E_0\left(1 + \Delta\alpha_i \hat{e}^I_i\right)$, ($i$=1,2,...,5) with midpoint value $E_0 = 2.1\times 10^8\ \text{kN}/\text{m}^2$ and deviation amplitude $\Delta\alpha_i = \Delta\alpha$ satisfying the condition $\Delta\alpha < 1$. The chimney is subjected to

turbulent wind loads modeled as nodal forces $F_{x,i}(z_i,t)$ in the along-wind direction applied to each node located at different height $z_i = i\,L$ (i=1,2,...,5), and expressed in the form reported in Eq. (53). The tributary area A_i of the i-th FE node is $A_i = 7.395\ \mathrm{m}^2$ for $i = 1,2,..,4$ and $A_5 = 3.6975\ \mathrm{m}^2$.

For this class of structures, the solution of the eigenproblem in Eq. (22) provides only two eigenvalues different from zero, i.e. $p_i = 2$, so that the spectral decomposition of the matrix $\mathbf{K}_i$ yields $\mathbf{K}_i = \sum_{\ell=1}^{2} \lambda_i^{(\ell)} \mathbf{v}_i^{(\ell)} \mathbf{v}_i^{(\ell)\mathrm{T}}$ (see Eq. (20)).

Figures 6 and 7 show the *LB* and *UB* of the *interval reliability function* of the *extreme value* processes of the horizontal displacements of nodes 1 and 5 of the chimney structure, $Y^I_{\max}(T) = U^I_{1\max}(T)$ and $Y^I_{\max}(T) = U^I_{5\max}(T)$, for two different levels of uncertainty, namely $\Delta\alpha = 0.05$ and $\Delta\alpha = 0.1$, and $T = 1000T_0$. The estimates of the *LB* and *UB* provided by the proposed procedure are contrasted with the exact bounds obtained by applying the *vertex method* which involves 2^5 stochastic analyses. For completeness, the nominal *CDFs*, $L^{(0)}_{U_{1\max}}(b,T)$ and $L^{(0)}_{U_{5\max}}(b,T)$, are also plotted. It is worth noting that for $\Delta\alpha = 0.05$ (see Figs. 6a and 7a), the proposed *UB* and *LB* of the *CDF* are almost coincident with the exact ones. Furthermore, as shown in Figs. 6b and 7b, very accurate estimates of the bounds of the *CDF* are also obtained for larger deviation amplitudes of the interval Young's moduli, say $\Delta\alpha = 0.1$, especially in regard of the large width of the interval itself. Finally, as observed in the previous example, the width of the region of the *interval reliability functions* increases when larger uncertainty levels are considered. The gap between the nominal value and the *LB* of the interval *CDF* implies that the actual structural performance may seriously worsens due to parameters uncertainty.

The accuracy of the proposed procedure for structural reliability analysis of the chimney structure is measured also in terms of the interval index, $\beta^I_{Y_{\max}}(T)$, introduced in Eq. (57). Also for

this case study, the expressions derived for the bounds of the interval mean-value $\mu^I_{Y_{\max}}(T)$ and standard deviation $\sigma^I_{Y_{\max}}(T)$ reported in Eqs. (59a,b) and (60a,b) hold true.

Table 2 lists the bounds of the interval index $\beta^I_{Y_{\max}}(T) = \beta^I_{U_{5\max}}(T)$ of the *extreme value* process $Y^I_{\max}(T) = U^I_{5\max}(T)$ of the horizontal displacement of node 5 of the chimney structure under study pertaining to four different critical values b_0 together with the absolute percentage errors evaluated according to Eq. (61). Also for the chimney structure, the accuracy of the proposed approach is confirmed by a percentage error $\varepsilon_\beta(\%)$ which does not exceed the 6.4% in the region of interest.

Finally, the c.i.u. (in percentage) of the *extreme value process* $Y^I_{\max}(T) = U^I_{5\max}(T)$ for the chimney structure turns out to be about 2.34% for a threshold $b_0 = 0.12$ m and $\Delta\alpha = 0.1$, while values of the c.i.u. of about 0.334 %, 0.039% and 0.004% are obtained for different thresholds, say $b_0 = 0.13, 0.14$ and 0.15 m, respectively. Also in this case, the dispersion of the interval *CDF* around the midpoint value decreases as larger threshold values are considered.

7 CONCLUSIONS

Structural reliability assessment of linear discretized structures with interval parameters subjected to stationary Gaussian random excitation has been addressed. Within the context of the *first passage failure* model, under the Poisson assumption of independent up-crossings, an efficient method for determining the region of the *interval reliability function* of a selected response process has been proposed. The key idea is to evaluate the lower bound and upper bound of the *interval reliability function* by seeking the minimum and maximum among the *reliability functions* corresponding to appropriate combinations of the bounds of the interval mean-value and spectral moments of zero- and second-order of the response process. In particular, it has been demonstrated that only two combinations need to be explored for each bound of the *interval reliability function*, regardless of the number of uncertain structural parameters. The strength of the method basically lies in the

derivation of approximate expressions of the bounds of the interval mean-value and spectral moments involved in the aforementioned combinations by applying the *improved interval analysis via extra unitary interval* in conjunction with the so-called *Interval Rational Series Expansion*.

The proposed approach turns out to be much more efficient from a computational point of view than a crude combinatorial procedure, i.e. the *vertex method*, which requires as many stochastic analyses as are the combinations of the bounds of the interval structural parameters. Furthermore, for structures with a large number of uncertainties, the computational efficiency can be greatly enhanced by performing a preliminary sensitivity analysis.

Another remarkable feature of the presented method is that the only source of approximation affecting the accuracy of the results lies in the evaluation of the bounds of the interval mean-value and spectral moments of the response by means of the *interval analysis via extra unitary interval* and *Interval Rational Series Expansion*. This circumstance guarantees accurate estimates of the bounds of the *interval reliability function* even for relatively large uncertainty levels which, in general, cannot be handled by other approximate methods like the one based on *first-order interval Taylor series expansion*, recently proposed by the authors [31].

For validation purpose, numerical results concerning a truss structure and a steel chimney with uncertain Young's modulus under wind excitations have been presented. The accuracy and computational efficiency of the proposed procedure have been demonstrated by appropriate comparisons with the *vertex method*. Such comparisons have shown the accuracy of the proposed estimates of the bounds of the *interval reliability function* and related quantities, even for relatively large uncertainty levels, despite the required computational effort is much lower than the one associated to the *vertex method*. Furthermore, numerical results have highlighted the usefulness of interval-based estimates of structural reliability for design purposes.

REFERENCES

[1] A. Der Kiureghian, Analysis of structural reliability under parameter uncertainties, Probab. Eng. Mech. 23 (2008) 351–358.

[2] A. Der Kiureghian, O. Ditlevsen, Aleatory or epistemic? Does it matter? Struct. Saf. 31 (2009) 105–112.

[3] B. Goller, H.J. Pradlwarter, G.I. Schüeller, Reliability assessment in structural dynamics, J. Sound Vib. 332 (2013) 2488–2499.

[4] Y. Ben-Haim, A non-probabilistic concept of reliability, Struct. Saf. 14(4) (1994) 227-245.

[5] I. Elishakoff, Essay on uncertainties in elastic and viscoelastic structures: From A. M. Freudenthal's criticisms to modern convex modeling, Comput. Struct. 56(6) (1995) 871–895.

[6] I. Elishakoff, M. Ohsaki, Optimization and Anti-Optimization of Structures under Uncertainty, Imperial College Press, London, 2010.

[7] R. E. Moore, Interval Analysis, Prentice-Hall, Englewood Cliffs, 1966.

[8] R.E. Moore, R.B. Kearfott, M.J. Cloud, Introduction to Interval Analysis, SIAM, Philadelphia, 2009.

[9] R.C. Penmetsa, R.V. Grandhi, Efficient estimation of structural reliability for problems with uncertain intervals, Comput. Struct. 80 (2002) 1103–1112.

[10] Z. Qiu, D. Yang, I. Elishakoff, Probabilistic interval reliability of structural systems, Int. J. Solids Struct. 45 (2008) 2850–2860.

[11] H. Zhang, R.L. Mullen, R.L Muhanna,. Interval Monte Carlo methods for structural reliability, Struct. Saf. 32 (2010) 183-190.

[12] J. E. Hurtado, D.A. Alvarez, The encounter of interval and probabilistic approaches to structural reliability at the design point, Comput. Methods Appl. Mech. Eng. 225–228 (2012) 74–94.

[13] H. Zhang, Interval importance sampling method for finite element-based structural reliability assessment under parameter uncertainties, Struct. Saf. 38 (2012) 1–10.

[14] J. E. Hurtado, Assessment of reliability intervals under input distributions with uncertain parameters, Probab. Eng. Mech. 32 (2013) 80–92.

[15] C. Jiang, R.G. Bi, G.Y. Lu, X. Han, Structural reliability analysis using non-probabilistic convex model, Comput. Methods Appl. Mech. Eng. 254 (2013) 83–98.

[16] H. Zhang, H. Dai, M. Beer, W. Wang, Structural reliability analysis on the basis of small samples: An interval quasi-Monte Carlo method, Mech. Syst. Signal Pr. 37 (2013) 137–151.

[17] D. A. Alvarez, J. E. Hurtado, An efficient method for the estimation of structural reliability intervals with random sets, dependence modeling and uncertain inputs, Comput. Struct. 142 (2014) 54–63.

[18] Y.C. Bai, X. Han, C. Jiang, R.G. Bi, A response-surface-based structural reliability analysis method by using non-probability convex model, Appl. Math. Model. 38 (2014) 3834–3847.

[19] E. Jahani, R.L. Muhanna, M.A. Shayanfar, Barkhordari, M.A. Reliability assessment with fuzzy random variables using Interval Monte Carlo Simulation, Comput.-Aided Civil Infrastruct Eng. 29 (2014) 208–220.

[20] C. Jiang, B.Y. Ni, X. Han, Y.R. Tao, Non-probabilistic convex model process: A new method of time-variant uncertainty analysis and its application to structural dynamic reliability problems, Comput. Methods Appl. Mech. Eng. 268 (2014) 656–676.

[21] T. Aven, Interpretations of alternative uncertainty representations in a reliability and risk analysis context, Reliab. Eng. Syst. Safe. 96 (2011) 353–360.

[22] M. Beer, Y. Zhang, S.T. Quek, K.K. Phoon, Reliability analysis with scarce information: comparing alternative approaches in a geotechnical engineering context, Struct. Saf. 41 (2013) 1–10.

[23] P.R. Adduri, R.C. Penmetsa, System reliability analysis for mixed uncertain variables, Struct. Saf. 31 (2009) 375–382.

[24] J. Wang, Z. Qiu, The reliability analysis of probabilistic and interval hybrid structural system, Appl. Math. Model. 34 (2010) 3648–3658.

[25] U. Alibrandi, C. G. Koh, First-order reliability method for structural reliability analysis in the presence of random and interval variables, ASME J. Risk Uncertainty Part B 1(4), 041006 (2015), (10 pages).

[26] Z. Hu, X. Du, A random field approach to reliability analysis with random and interval variables, ASME J. Risk Uncertainty Part B 1(4), 041005 (2015), (11 pages),

[27] J. Ma, W. Gao, P. Wriggers, T. Wu, S. Sahraee, The analyses of dynamic response and reliability of fuzzy-random truss under stationary stochastic excitation, Comput. Mech. 45 (2010) 443–455.

[28] D. Moens, D. Vandepitte, A survey of non-probabilistic uncertainty treatment in finite element analysis, Comput. Methods Appl. Mech. Eng. 194 (2005) 1527–1555.

[29] L.D. Lutes, S. Sarkani, Stochastic Analysis of Structural and Mechanical Vibrations, Prentice-Hall, Upper Saddle River, 1997.

[30] J. Li, J.B. Chen, Stochastic Dynamics of Structures, John Wiley & Sons, Singapore, 2009.

[31] G. Muscolino, R. Santoro, A. Sofi, Explicit reliability sensitivities of linear structures with interval uncertainties under stationary stochastic excitations, Struct. Saf. 52, Part B (2015) 219–232.

[32] D.M. Do, W. Gao, C. Song, S. Tangaramvong, Dynamic analysis and reliability assessment of structures with uncertain-but-bounded parameters under stochastic process excitations, Reliab. Eng. Syst. Safe. 132, (2014) 46–59.

[33] G. Muscolino, A. Sofi, Stochastic analysis of structures with uncertain-but-bounded parameters via improved interval analysis, Probab. Eng. Mech. 28 (2012) 152-163.

[34] G. Muscolino, A. Sofi, Bounds for the stationary stochastic response of truss structures with uncertain-but-bounded parameters, Mech. Syst. Signal Pr. 37 (2013) 163-181.

[35] G. Muscolino, R. Santoro, A. Sofi, Explicit sensitivities of the response of discretized structures under stationary random processes, Probab. Eng. Mech. 35 (2014) 82-95.

[36] G. Muscolino, R. Santoro, A. Sofi, Explicit frequency response functions of discretized structures with uncertain parameters, Comput. Struct. 133 (2014) 64–78.

[37] E.H. Vanmarcke, On the distribution of the first-passage time for normal stationary random processes, J. Appl. Mech. ASME 42, (1975) 215-220.

[38] S. O. Rice, Mathematical analysis of random noise, Bell Syst. Tech. J. 23 (1944) 282–332.

[39] E.H. Vanmarcke, Properties of spectral moments with applications to random vibration, J. Eng. Mech. ASCE 98 (1972) 425-446.

[40] G. Falsone, G. Ferro, An exact solution for the static and dynamic analysis of FE discretized uncertain structures, Comput. Methods Appl. Mech. Eng. 196 (2007) 2390–2400.

[41] F. Yamazaki, M. Shinozuka, G. Dasgupta, Neumann expansion for stochastic finite element analysis, J. Eng. Mech. ASCE 114(8) (1988) 1335–1354.

[42] R.G. Ghanem, P.D. Spanos, Stochastic Finite Elements: A Spectral Approach, Springer-Verlag, New York, 1991.

[43] N. Impollonia, G. Muscolino, Interval analysis of structures with uncertain-but-bounded axial stiffness, Comput. Methods Appl. Mech. Eng. 200 (21-22) (2011) 1945–1962.

[44] G. Falsone, N. Impollonia, A new approach for the stochastic analysis of finite element modelled structures with uncertain parameters, Comput. Methods Appl. Mech. Eng. 191(44) (2002) 5067-5085.

[45] E. Simiu, R. Scanlan, Wind Effects on Structures, John Wiley & Sons, New York, 1996.

[46] A.G. Davenport, The spectrum of horizontal gustiness near the ground in high winds, Q. J. Roy. Meteorol. Soc. 87 (1961) 194–211.

[47] G. Davenport, Note on the distribution of the largest value of a random function with application to gust loading, Inst. Civil Eng. Proc. 28 (1964) 187-196.

Figure Captions

Fig. 1. Flow-chart of the proposed method for interval reliability analysis.

Fig. 2. 25-bar truss structure under wind excitation.

Fig. 3. Comparison between the exact and proposed *UB* and *LB* of the *CDF* of the *extreme value* process $Y^I_{\max}(T)=U^I_{1\max}(T)$ of the horizontal displacement of node 1 of the truss structure $\left(T=1000T_0\right)$ with interval Young's moduli $E^I_i=E_0\left(1+\Delta\alpha\,\hat{e}^I_i\right)$ of the diagonal bars for a) $\Delta\alpha=0.1$ and b) $\Delta\alpha=0.15$.

Fig. 4. Comparison between the exact and proposed *UB* and *LB* of the *CDF* of the *extreme value* process $Y^I_{\max}(T)=U^I_{9\max}(T)$ of the horizontal displacement of node 9 of the truss structure $\left(T=1000T_0\right)$ with interval Young's moduli $E^I_i=E_0\left(1+\Delta\alpha\,\hat{e}^I_i\right)$ of the diagonal bars for a) $\Delta\alpha=0.1$ and b) $\Delta\alpha=0.15$.

Fig. 5. Chimney structure and FE model.

Fig. 6. Comparison between the exact and proposed *UB* and *LB* of the *CDF* of the *extreme value* process $Y^I_{\max}(T)=U^I_{1\max}(T)$ of the horizontal displacement of node 1 of the chimney structure $\left(T=1000T_0\right)$ with interval Young's moduli $E^I_i=E_0\left(1+\Delta\alpha\,\hat{e}^I_i\right)$ for a) $\Delta\alpha=0.05$ and b) $\Delta\alpha=0.1$.

Fig. 7. Comparison between the exact and proposed *UB* and *LB* of the *CDF* of the *extreme value* process $Y^I_{\max}(T)=U^I_{5\max}(T)$ of the horizontal displacement of node 5 of the chimney structure $\left(T=1000T_0\right)$ with interval Young's moduli $E^I_i=E_0\left(1+\Delta\alpha\,\hat{e}^I_i\right)$ for a) $\Delta\alpha=0.05$ and b) $\Delta\alpha=0.1$.

Fig. 8. Professor Giuseppe Muscolino

Fig.9. Dr. Roberta Santoro

Fig.10. Dr. Alba Sofi

Table Captions

Table 1. Index $\beta^I_{U_{9\max}}(T)$ bounds of the *extreme value* process $Y^I_{\max}(T) = U^I_{9\max}(T)$ of the horizontal displacement of node 9 of the truss structure with interval Young's moduli $E^I_i = E_0\left(1 + \Delta\alpha\,\hat{e}^I_i\right)$ of the diagonal bars for $\Delta\alpha = 0.1$.

Table 2. Index $\beta^I_{U_{5\max}}(T)$ bounds of the *extreme value* process $Y^I_{\max}(T) = U^I_{5\max}(T)$ of the horizontal displacement of node 5 of the chimney structure with interval Young's moduli $E^I_i = E_0\left(1 + \Delta\alpha\,\hat{e}^I_i\right)$ for $\Delta\alpha = 0.1$.

Curriculum Vitae

Giuseppe Muscolino since 1990 is Professor in Structural Engineering. Today he serves as professor of Structural Dynamics at the University of Messina (Italy). Prior to that he served as Researcher, Associate Professor and Professor of Structural Mechanics at the University of Palermo. He carried out numerous organizing duties. He serves on the Editorial Board of several Journals. He supervised Ph.D students at the University of Catania, Messina and Palermo. He held several invited lectures. He is author or coauthor of 4 books and of numerous scientific articles concerning: deterministic and stochastic dynamics of structures, mechanics of structures with uncertain parameters.

Roberta Santoro, PhD starting from December 2010 is Assistant Professor of Structural Mechanics. Today she serves as professor of Modeling and Dynamics of Structures at the University of Messina (Italy). Prior to that she served as Research Assistant at the University of Palermo. She is author and coauthor of scientific articles concerning deterministic and stochastic dynamics of structures, fractional calculus and strength of materials problems.

Alba Sofi is Assistant Professor of Structural Mechanics at University "Mediterranea" of Reggio Calabria (Italy). She received her Ph.D degree in Structural Engineering from the University of Palermo in 2002 (Italy). In 2004, she was appointed as Visiting Scholar at Rice University (Houston, USA). She is active referee for several International Journals. She serves as Guest Editor of the *ASCE-ASME Journal of Risk and Uncertainty in Engineering Systems*. Her primary research interests focus on: stochastic dynamics; probabilistic and non-probabilistic approaches in uncertainty quantification with specific expertise in interval analysis; bridge-vehicle dynamic interaction; cable dynamics; non-local elasticity theory.

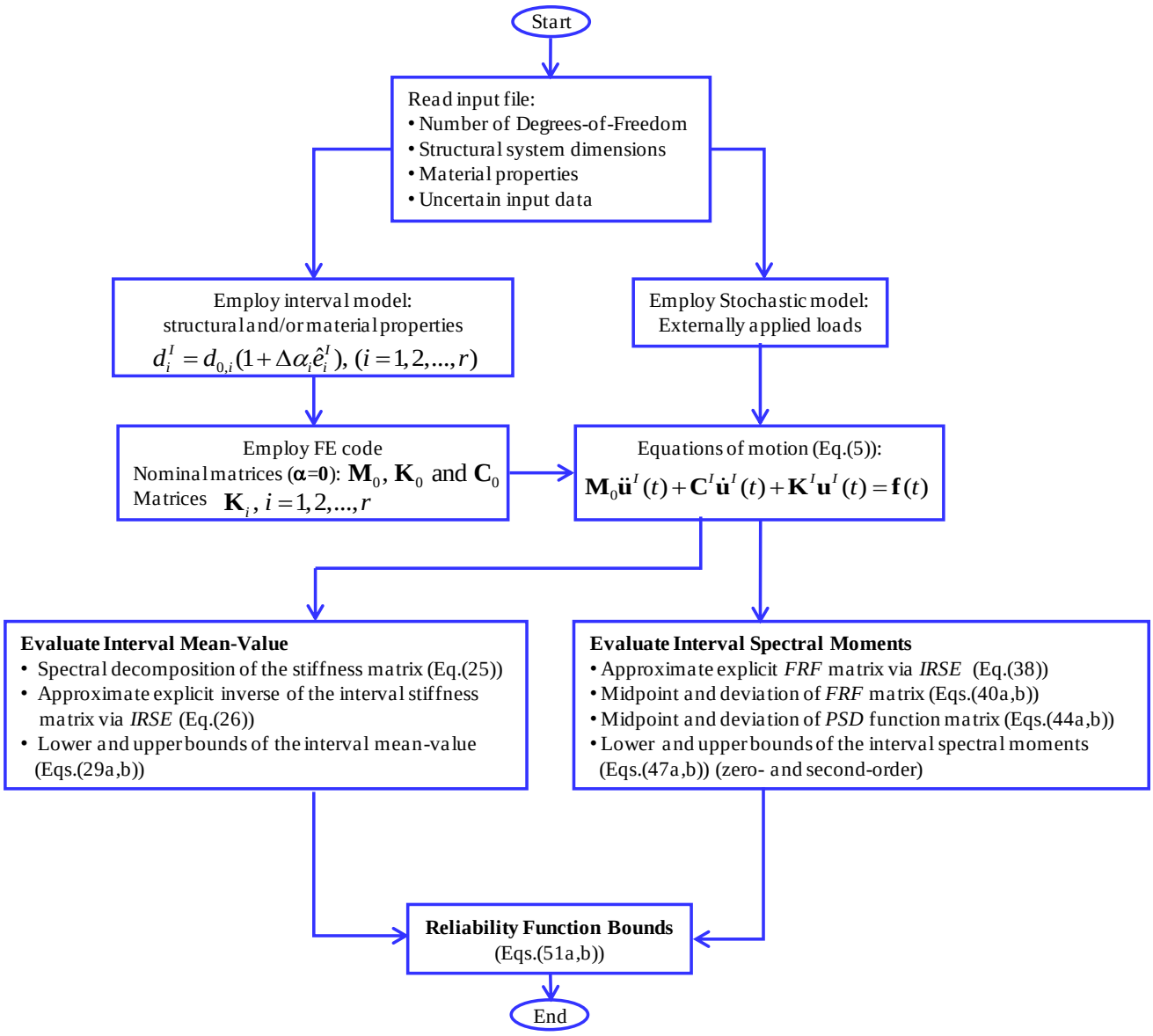

Figure 1. Flow-chart of the proposed method for interval reliability analysis.

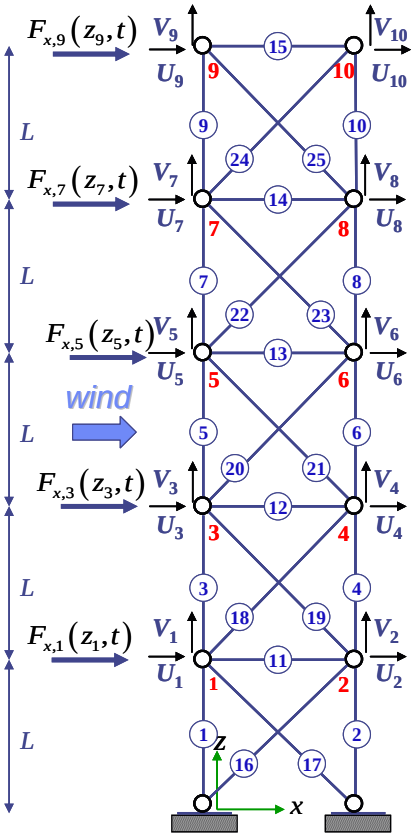

Figure 2. 25-bar truss structure under wind excitation.

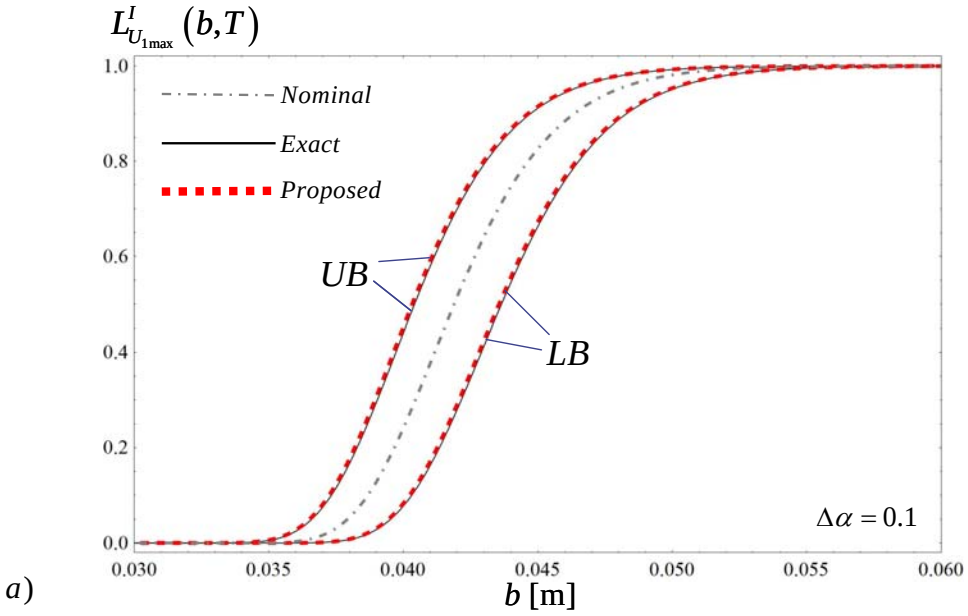

a)

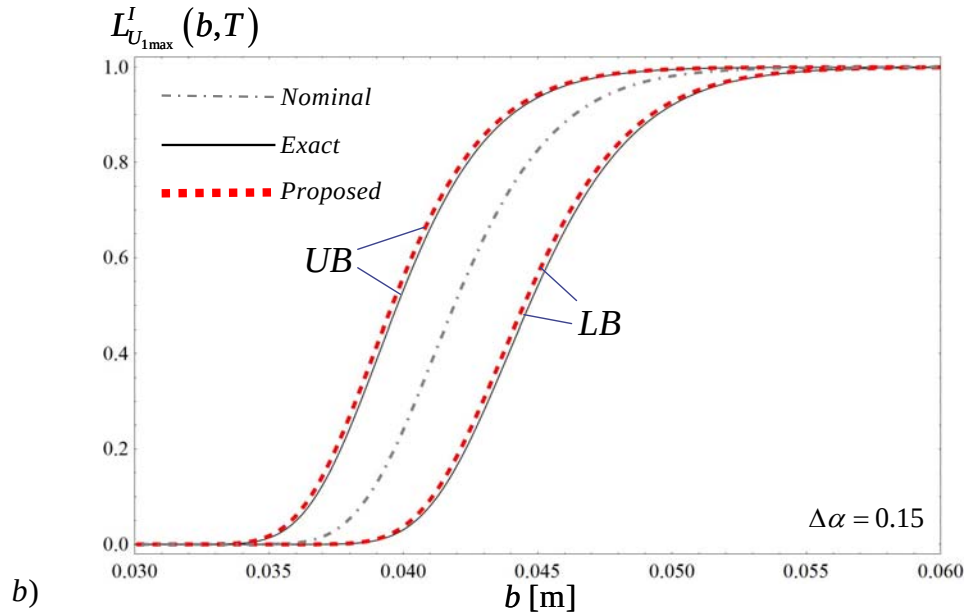

b)

Figure 3. Comparison between the exact and proposed *UB* and *LB* of the *CDF* of the *extreme value* process $Y^I_{\max}(T) = U^I_{1\max}(T)$ of the horizontal displacement of node 1 of the truss structure $(T = 1000T_0)$ with interval Young's moduli $E^I_i = E_0\left(1 + \Delta\alpha\,\hat{e}^I_i\right)$ of the diagonal bars for a) $\Delta\alpha = 0.1$ and b) $\Delta\alpha = 0.15$.

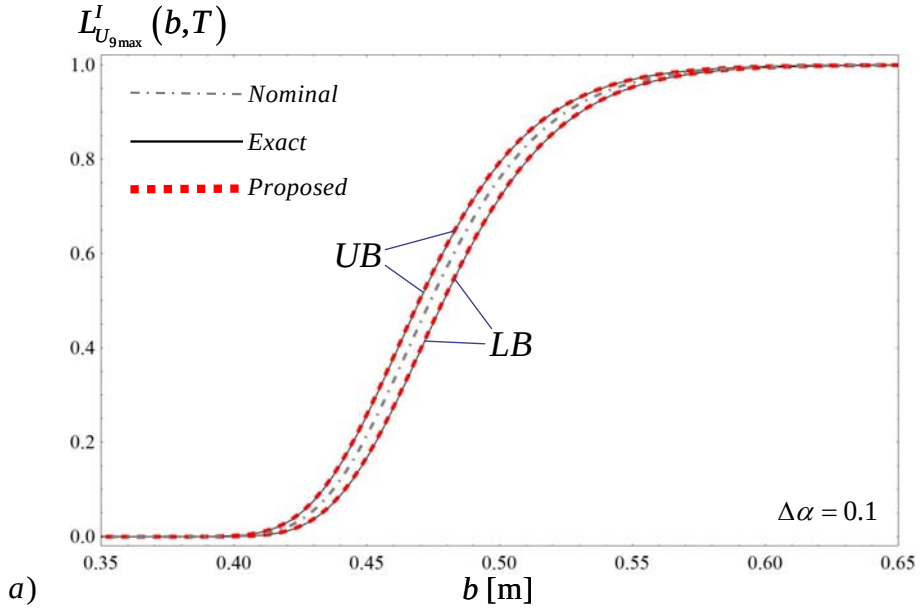

a)

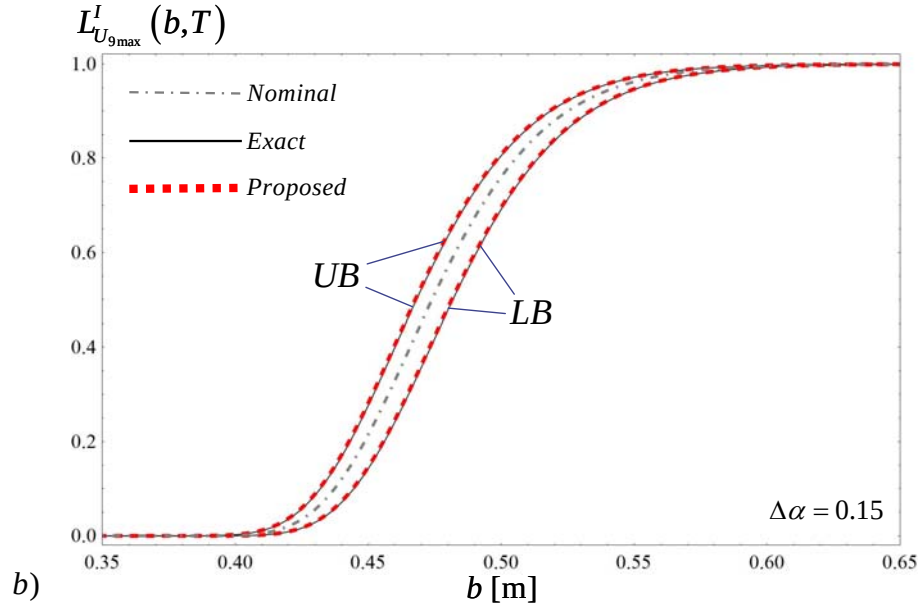

b)

Figure 4. Comparison between the exact and proposed *UB* and *LB* of the *CDF* of the *extreme value* process $Y^I_{\max}(T) = U^I_{9\max}(T)$ of the horizontal displacement of node 9 of the truss structure $(T = 1000T_0)$ with interval Young's moduli $E^I_i = E_0\left(1 + \Delta\alpha\,\hat{e}^I_i\right)$ of the diagonal bars for a) $\Delta\alpha = 0.1$ and b) $\Delta\alpha = 0.15$.

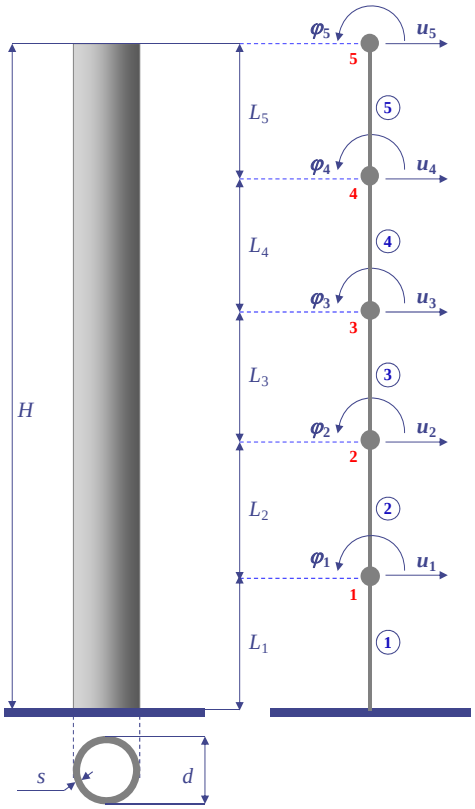

Figure 5. Chimney structure and FE model.

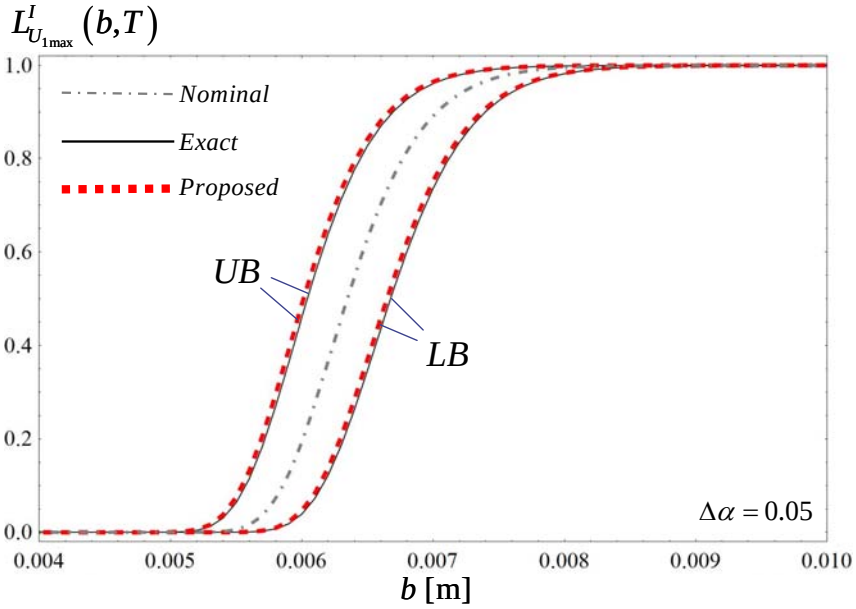

a)

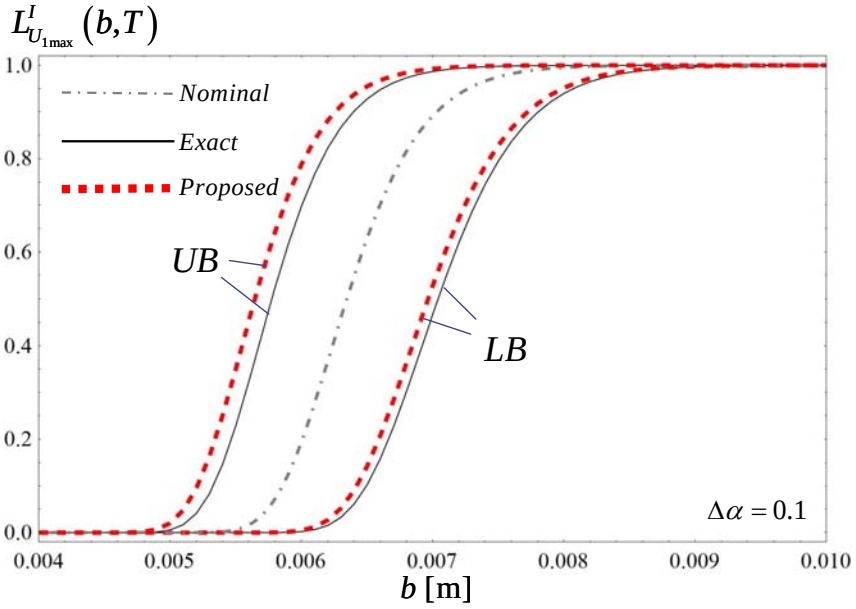

b)

Figure 6. Comparison between the exact and proposed *UB* and *LB* of the *CDF* of the *extreme value* process $Y^I_{\max}(T) = U^I_{1\max}(T)$ of the horizontal displacement of node 1 of the chimney structure $(T = 1000T_0)$ with interval Young's moduli $E^I_i = E_0\left(1 + \Delta\alpha\,\hat{e}^I_i\right)$ for a) $\Delta\alpha = 0.05$ and b) $\Delta\alpha = 0.1$.

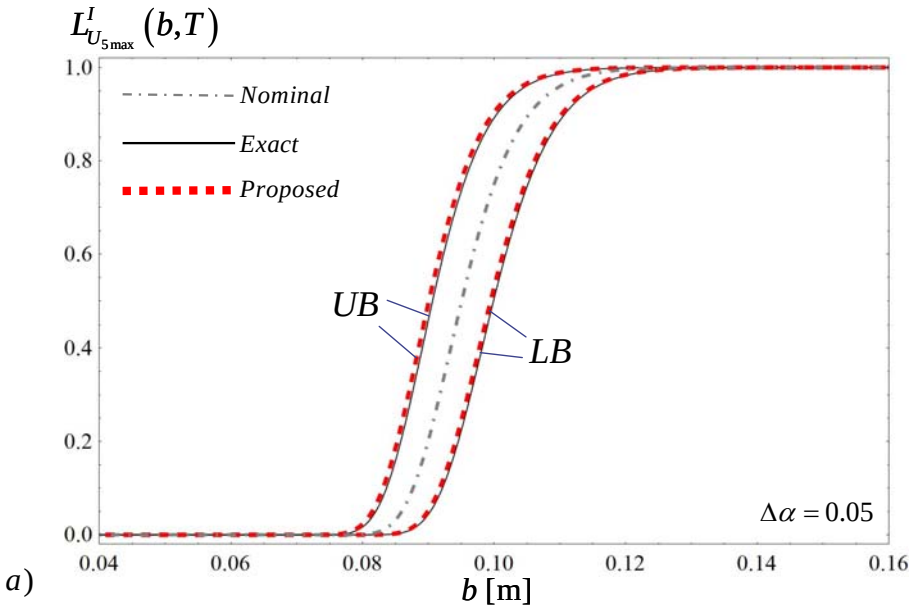

a)

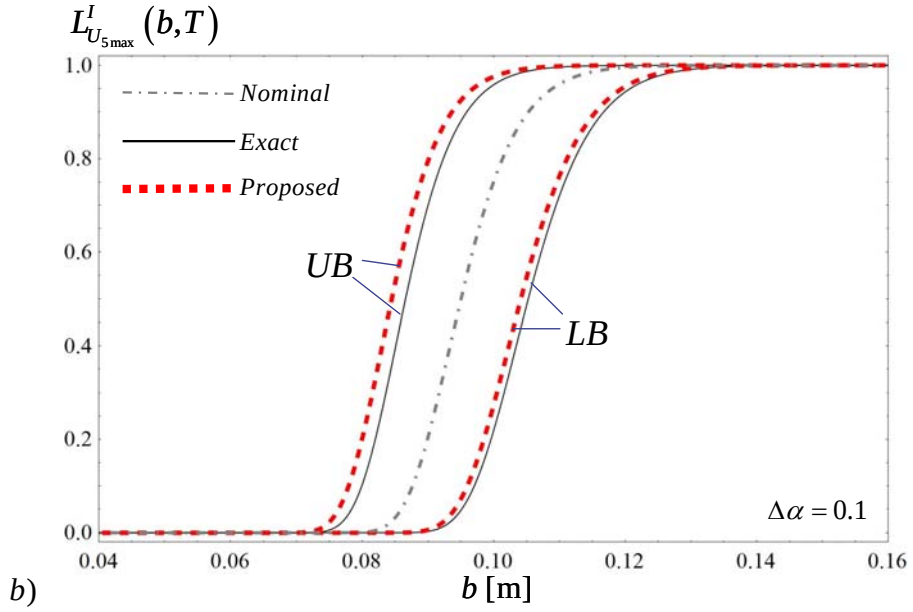

b)

Figure 7. Comparison between the exact and proposed *UB* and *LB* of the *CDF* of the *extreme value* process $Y^I_{\max}(T) = U^I_{5\max}(T)$ of the horizontal displacement of node 5 of the chimney structure $(T = 1000T_0)$ with interval Young's moduli $E^I_i = E_0\left(1 + \Delta\alpha\,\hat{e}^I_i\right)$ for a) $\Delta\alpha = 0.05$ and b) $\Delta\alpha = 0.1$.

Figure 8. Professor Giuseppe Muscolino

Figure 9. Dr. Roberta Santoro

Figure 10. Dr. Alba Sofi

Table 1. Index $\beta^I_{U_{9\max}}$ bounds of the *extreme value* process $Y^I_{\max}(T) = U^I_{9\max}(T)$ of the horizontal displacement of node 9 of the truss structure with interval Young's moduli $E^I_i = E_0\left(1 + \Delta\alpha\,\hat{e}^I_i\right)$ of the diagonal bars for $\Delta\alpha = 0.1$

	Index $\beta^I_{U_{9\max}}$ bounds			
b_0	$\underline{\beta}_{U_{9\max}}$ (exact)	$\underline{\beta}_{U_{9\max}}$ (proposed)	$\overline{\beta}_{U_{9\max}}$ (exact)	$\overline{\beta}_{U_{9\max}}$ (proposed)
0.58	5.2157	5.2213	5.5195	5.5259
ε_β(%)	0.109		0.116	
0.60	5.7315	5.7374	6.0469	6.0536
ε_β(%)	0.102		0.110	
0.62	6.2474	6.2534	6.5743	6.5812
ε_β(%)	0.097		0.104	
0.64	6.7633	6.7695	7.1018	7.1089
ε_β(%)	0.092		0.010	

Table 2. Index $\beta^I_{U_{5\max}}$ bounds of the *extreme value* process $Y^I_{\max}(T) = U^I_{5\max}(T)$ of the horizontal displacement of node 5 of the chimney structure with interval Young's moduli $E^I_i = E_0\left(1+\Delta\alpha\,\hat{e}^I_i\right)$ for $\Delta\alpha = 0.1$

	Index $\beta^I_{U_{5\max}}$ bounds			
b_0	$\underline{\beta}_{U_{5\max}}$ (exact)	$\underline{\beta}_{U_{5\max}}$ (proposed)	$\overline{\beta}_{U_{5\max}}$ (exact)	$\overline{\beta}_{U_{5\max}}$ (proposed)
0.12	4.2789	4.4139	7.4813	7.9566
ε_β(%)	3.154		6.353	
0.13	5.4313	5.5674	8.9273	9.4343
ε_β(%)	2.505		5.678	
0.14	6.5837	6.7208	10.3734	10.9120
ε_β(%)	2.083		5.192	
0.15	7.7361	7.8743	11.8194	12.3896
ε_β(%)	2.505		4.824	